Supporting Information (SI)

Dehydrogenative Azolation of Arenes in a Microflow Electrochemical Reactor

Laura Buglioni,[1] Marko Beslać,[1] Timothy Noël[2,*]

[1]Micro Flow Chemistry and Synthetic Methodology, Department of Chemical Engineering and Chemistry, Eindhoven University of Technology, Het Kranenveld, Bldg 14 –Helix, 5600 MB, Eindhoven, The Netherlands.

[2]Homogeneous, Supramolecular and Bio-inspired Catalysis Group (HomKat), van 't Hoff Institute for Molecular Sciences (HIMS), Universiteit van Amsterdam (UvA), Science Park 904, 1098 XH, Amsterdam, The Netherlands.

*Corresponding author, e-mail: t.noel@uva.nl

Table of Contents

1. General information S3
2. Reaction optimization S4
3. Stability of the system S9
4. Reaction Scale Up S10
5. Unsuccessful substrates S11
6. Cleaning procedure S12
7. NMR spectra S13
8. References S35

1. General information

All reagents and solvents were used as received without further purification. Reagents and solvents were bought from Sigma Aldrich, TCI and Fluorochem. Technical solvents were bought from VWR International and Biosolve and were used as received. All capillary tubing and microfluidic fittings were purchased from IDEX Health & Science. Disposable syringes were from BD Discardit II® or NORM-JECT®, purchased from VWR Scientific. Syringe pumps were purchased from Chemix Inc. model Fusion 200 Touch. The crude products were purified by flash column chromatography on silica gel (60, F254, Merck). TLC analysis was performed using Silica on aluminum foils TLC plates (F254, Supelco Sigma-Aldrich™) with visualization under ultraviolet light (254 nm and 365 nm). ^{1}H (400 MHz) and ^{13}C (100 MHz) spectra were recorded on ambient temperature using a Bruker-Avance 400. ^{1}H NMR and ^{13}C NMR spectra are reported in parts per million (ppm) downfield relative to $CDCl_3$ (7.26 ppm and 77.16 ppm, respectively) unless stated otherwise. NMR spectra uses the following abbreviations to describe the multiplicity: s = singlet, d = doublet, t = triplet, q = quartet, p = pentet, h = hextet, hept = heptet, m = multiplet, dd = double doublet, td = triple doublet. NMR data was processed using the MestReNova 11.0.4. Known products were characterized by comparing to the corresponding ^{1}H NMR and ^{13}C NMR from literature. High resolution mass spectra were recorded by using an Agilent Technologies 6220AAccurate-Mass TOF LC/MS spectrometer equipped with a multimode ESI/APCI ionization source. GC analyses were performed on a GC-MS combination (Shimadzu GC-2010 Plus coupled to a Mass Spectrometer; Shimadzu GCMS-QP 2010 Ultra) with an auto sampler unit (AOC-20i, Shimadzu) and GC-FID(Shimadzu GC-2010) with an auto sampler unit (AOC-20i, Shimadzu). The names of all products were generated using the PerkinElmer ChemBioDraw Ultra v.18.0.0 software package.

For all electrochemical continuous-flow reactions, a homemade flow cell was used (Figure S1), together with a Velleman LABPS3005D power supply. The cell consists of a working electrode and a counter electrode, with a PTFE (Polytetrafluoroethylene) 0.25 mm thick gasket containing micro-channels in between. The material used for the electrodes were Stainless Steel electrode (316L) and Graphite AC-K800 premium Grade (purchased by AgieCharmilles). The active reactor volume is 700 µL. This results in an undivided electrochemical cell. In the cell, direct contact between the electrode surface and the reaction mixture is established. The reaction mixture is pumped through the system via syringe pump and is collected in a glass vial. All the technical data of the electrochemical microreactor are reported elsewhere.[1]

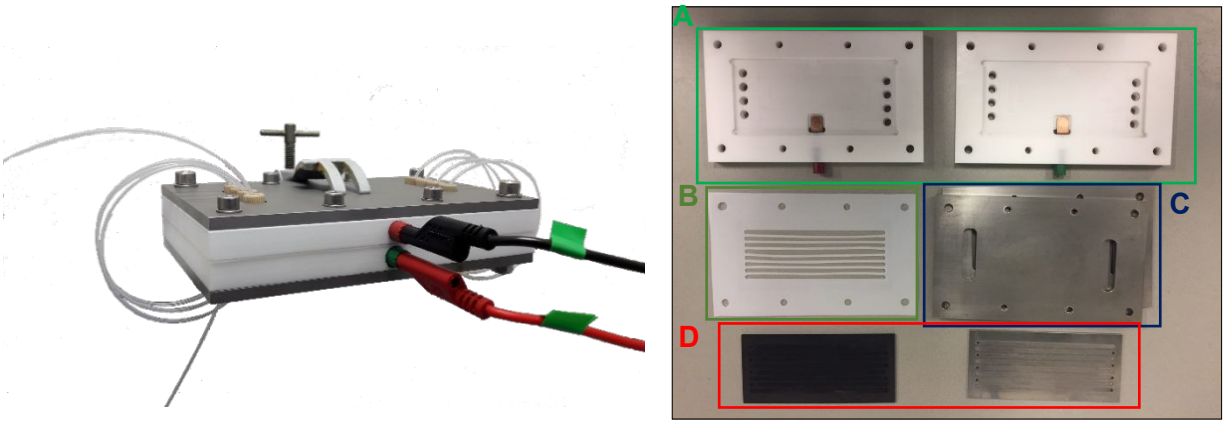

Figure S1: Left - Assembled Flow reactor. Right - Components of the electrochemical flow cell. A: PTFE electrode holders. B: PTFE gasket (8 channel configuration). C: Outer Stainless Steel plates. D: Electrodes (Left Graphite, Right Stainless Steel, 66 cm^2 each).

2. Reaction optimization

During the screening, the solution was pumped through the electrocell at a fixed flowrate of 0.07 mL·min^{-1} to give a residence time of 10 minutes. The current was varied from 10 to 70 mA (0.35-2.48 mA·cm^{-2}). After 2 residence times had elapsed and the reaction had reached steady state (20 minutes at 0.07 mL·min^{-1}), the corresponding potential was noted and a sample (0.1 mL) was collected in a vial and diluted with acetonitrile (1 mL). The diluted sample were analyzed using GC-FID. GC yields were calculated with an internal standard (diglyme).

2.1 Screening of the cathode material

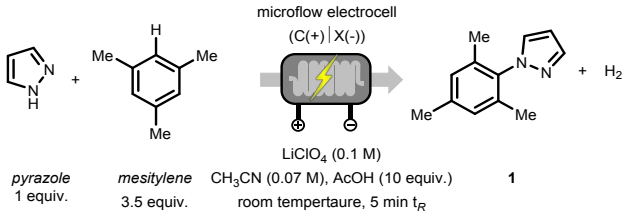

Table S1. Screening of two different materials for the cathode.

Entry	Cathode	Yield (%)
1	Stainless steel	46
2	Nickel	42

Reaction conditions: pyrazole (0.67 mmol), mesitylene (3.5 equiv.), $LiClO_4$ (0.1 M), CH_3COOH (10 equiv.), CH_3CN (10 mL, 0.07 M), C anode/Fe cathode, 0.35-2.48 mA·cm^{-2} (The best results refer to 0.71 mA·cm^{-2} which corresponds to 20 mA). Yield determined by GC-FID with diglyme as internal standard.

2.2 Screening of the residence time

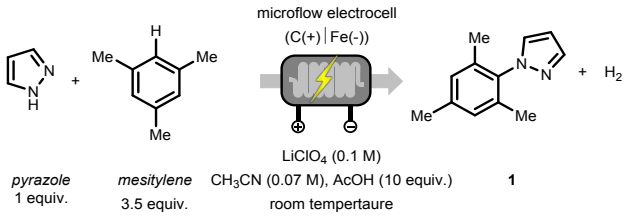

Table S2. Screening of the residence time.

Entry	Residence time (min)	Yield (%)
1	5	46
2	8	43
3	10	60

Reaction conditions: pyrazole (0.67 mmol), mesitylene (3.5 equiv.), $LiClO_4$ (0.1 M), CH_3COOH (10 equiv.), CH_3CN (10 mL, 0.07 M), C anode/Fe cathode, 0.35-2.48 mA·cm^{-2} (The best results refer to 0.71 mA·cm^{-2} which corresponds to 20 mA). Yield determined by GC-FID with diglyme as internal standard.

The yield benefits from a longer residence time screening (10 min vs. 5 min).

2.3 Screening of the supporting electrolyte

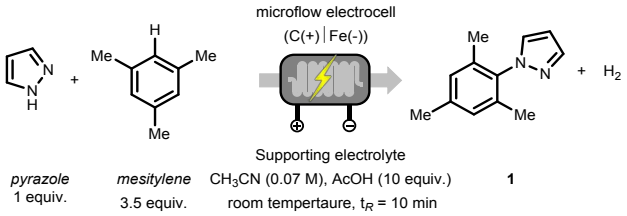

Table S3. Screening of the supporting electrolyte.

Entry	Supporting electrolyte	Yield (%)
1	$LiClO_4$ (0.05 M)	43
2	Me_4NBF_4 (0.05 M)	46
3	$LiClO_4$ (0.1 M)	60
4[a]	HFIP (10 equiv.)/DIPEA (1.0 equiv.)	-

Reaction conditions: pyrazole (0.67 mmol), mesitylene (3.5 equiv.), CH_3COOH (10 equiv.), CH_3CN (10 mL, 0.07 M), C anode/Fe cathode, 0.35-2.48 mA·cm^{-2} (The best results refer to 0.71 mA·cm^{-2} which corresponds to 20 mA). Yield determined by GC-FID with diglyme as internal standard. [a] No acetic acid was added

As $LiClO_4$ (0.05 M) and Me_4NBF_4 (0.05 M) were giving comparable results, we continued with $LiClO_4$, although at higher concentration. The electrolyte combination of HFIP with a tertiary amine[2] proved to be not efficient at all.

2.4 Stoichiometry of the transformation

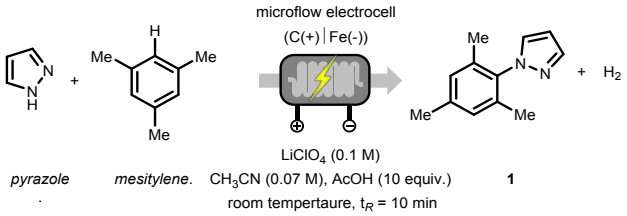

Table S4. Studies about the stoichiometry of the transformation.

Entry	Pyrazole (equiv.)	Mesitylene (equiv.)	Yield (%)
1	1.0	3.5	60
2	3.0	1.0	58
3[a]	3.0	1.0	43
4[a]	1.0	3.0	59
5	1.0	6.0	71

Reaction conditions: pyrazole (x equiv.), mesitylene (x equiv.), $LiClO_4$ (0.1 M), CH_3COOH (10 equiv.), CH_3CN (10 mL, 0.07 M), C anode/Fe cathode, 0.35-2.48 mA·cm^{-2} (The best results refer to 0.71 mA·cm^{-2} which corresponds to 20 mA). Yield determined by GC-FID with diglyme as internal standard. [a] In HFIP/CH_3OH 4:1

A change in the stoichiometry did not affect much the reaction outcome. However, in one of the experiments performed in a different solvent mixture (entry 3), it was possible to observe by GC-FID and by GC-MS a new peak corresponding to the difunctionalized mesitylene **A**. As expected, this peak was becoming more and more prominent with the increase of the applied current (and thus voltage). To avoid possible overoxidation side-products, we preferred to keep working with an excess or arene.

Moreover, we found out that increasing the excess of mesitylene up to 6.0 equiv. was very beneficial for the transformation (entry 5).

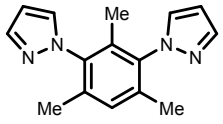

A

2.5 Screening of different solvents

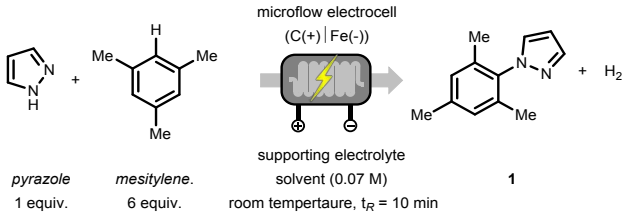

Table S5. Screening of the solvents.

Entry	Solvent	Supporting electrolyte	Yield (%)[a]	Yield (%)[b]
1	CH_3CN, AcOH (10 equiv.)	$LiClO_4$ (0.1 M)	71	60
2	HFIP/CH_3OH 4:1	$LiClO_4$ (0.1 M)	75	42
3	CF_3CH_2OH/CH_3OH 4:1	$LiClO_4$ (0.1 M)	70	71 (67)[c]
4	HFIP/CH_2Cl_2 7:3	Bu_4NPF_6 (0.05 M)	75	70 (67)[c]
5[d]	HFIP/CH_2Cl_2 7:3	Bu_4NPF_6 (0.05 M)	-	50
6[e]	HFIP/CH_2Cl_2 7:3	Bu_4NPF_6 (0.05 M)	-	0

Reaction conditions: pyrazole (0.67 mmol), mesitylene (6 equiv.), solvent (10 mL, 0.07 M), C anode/Fe cathode, 0.35-2.48 mA·cm^{-2} (The best results refer to 0.71 mA·cm^{-2} which corresponds to 20 mA). Yield determined by GC-FID with diglyme as internal standard. [a] Yield measured at the beginning of the collection of the sample. [b] Yield measured from the bulk sample which was collected over 75 min. [c] Numbers in brackets represent the yield after column chromatography. [d] The reaction was performed in an Electrasyn, 7.2 mA·cm^{-2}, 2.0 F, C anode/Fe cathode, 0.33 mmol scale, 1 h reaction time. [e] No current applied.

The results obtained in CH_3CN or in HFIP/CH_3OH 4:1 were very positive (entries 1 and 2). However, these solvent systems turned out not to be a very stable system, as shown in the last column. In fact, when collecting a sample over 75 min, the yield decreased with the time. The solvent system consisting of CF_3CH_2OH (TFE)/CH_3OH 4:1 performed better (entry 3), but its main limitation was its solubilizing power. In fact, when very apolar solid arenes were employed in excess, a suspension was formed. HFIP/CH_2Cl_2 7:3 was more promising as solvent mixture in terms of solubilizing power and was comparable in terms of yield and stability. It was necessary to switch the supporting electrolyte from 0.1 M $LiClO_4$ to 0.05 M Bu_4NPF_6 for solubility reasons, but without negative effects on the reaction outputs. In batch, the reaction was less efficient, even though with a longer time (entry 5). However, the current density is higher in batch than in flow. But it is important to note that when higher density were tested in flow, the yields dropped, probably because of the formation of by-products. The application of electrical current is necessary for the reaction to take place (entry 6).

2.6 Second screening of the residence time

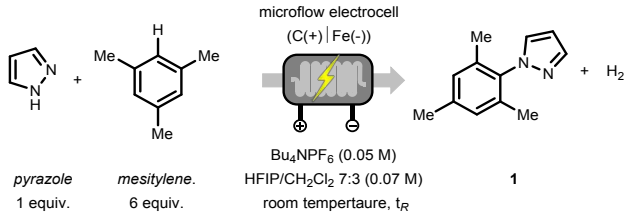

Table S6. Screening of the residence time.

Entry	residence time t_R (min)	F·mol^{-1}	Yield (%)[b]
1	5	1.3	37
2	10	2.6	71 (67)[c]
3	20	5.3	83

Reaction conditions: pyrazole (0.67 mmol), mesitylene (6 equiv.), solvent (10 mL, 0.07 M), C anode/Fe cathode, 0.35-2.48 mA·cm^{-2}. (The best results refer to 0.71 mA·cm-2 which corresponds to 20 mA). Yield determined by GC-FID with diglyme as internal standard. [c] Numbers in brackets represent the yield after column chromatography.

When the residence time is set at 5 min, the amount of charge provided with 20 mA is not sufficient for the transformation, which requires a minimum of 2 F·mol^{-1}. However, worse results were obtained at higher current densities.

The results obtained setting the residence time at 20 min is very good, but considering the yield oscillation during the flow reaction (see next section), we considered it comparable to the results obtained with t_R = 10 min, which ensure higher productivity (due to higher flow rate).

3. Stability of the system

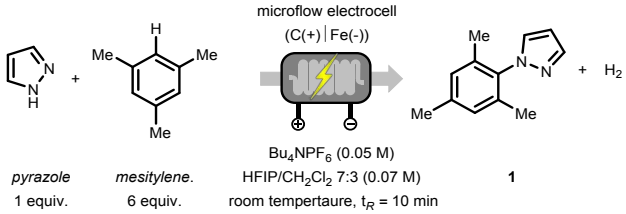

Table S7. Variation of the conversion and of the yield during time.

T (min)	Yield (%)	Conversion (%)
20	75	85
30	78	87
40	85	86
50	79	80
60	83	86
70	67	78
80	74	85
90	77	86
100	73	89
110	71	84
120	70	83

The reaction (20 mL) was performed under standard conditions for 120 min and samples were collected every 10 min, and analyzed with GC-FID (diglyme as internal standard)

We found out that after 70 min the yield and the conversion dropped, probably because of pollution of the electrodes. To overcome this issue, it was sufficient to rinse the electrodes with acetonitrile to restore its original activity.

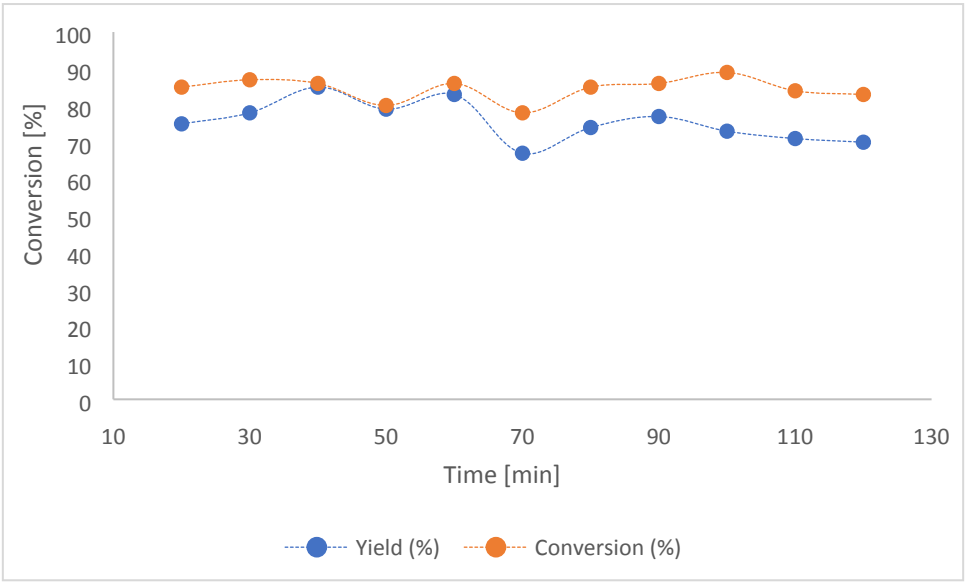

Figure S2. Variation of the conversion (y-axis) and of the yield (y-axis) over time (x-axis, in minutes). At 70 min a drop in conversion/yield can be observed. At that point, the electrodes were cleaned (see section 6) and afterwards the same reactivity could be observed.

4. Reaction Scale Up

Pyrazole (1.0 equiv., 3.35 mmol, 228 mg) was dissolved in a mixture of HFIP/CH_2Cl_2 7:3 (50 mL), together with Bu4NPF6 (0.05 M, 968 mg) and mesitylene (6.0 equiv., 0.864 $g \cdot mL^{-1}$, 2.8 mL), using a 50 mL volumetric flask (0.067 M). The mixture was swirled until homogeneous and placed in a 50 mL disposable syringes. The solution was pumped through the electrochemical setup with a fixed flow rate of 0.07 mL/min to give a residence time of 10 minutes in the active part of the reactor, equipped with a graphite anode, steel cathode divided by a 0.25 mm thick Teflon gasket. The first fraction was discarded after which a constant current of 20 mA was applied. Every hour, the reactor disassembled in order to properly clean the electrodes. After that, the flow of the reaction was started again. In total, 23.2 mL of solution were collected, corresponding to 1.5 mmol.

The crude mixture was concentrated under vacuum and was directly purified by flash column chromatography on silica gel (cyclohexane 100% to cyclohexane:EtOAc 95:5) to give 1-mesityl-1*H*-pyrazole (**1**) as a viscous brown oil in 75% yield (219 mg, 1.17 mmol)

5. Unsuccessful substrates

Azoles

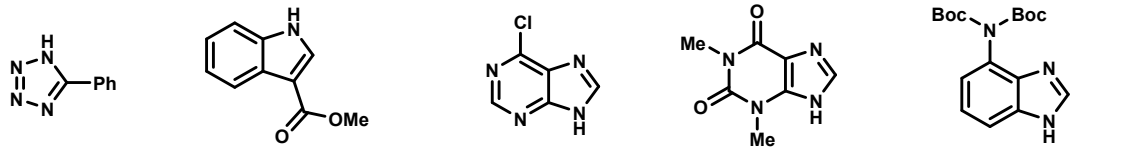

Arenes

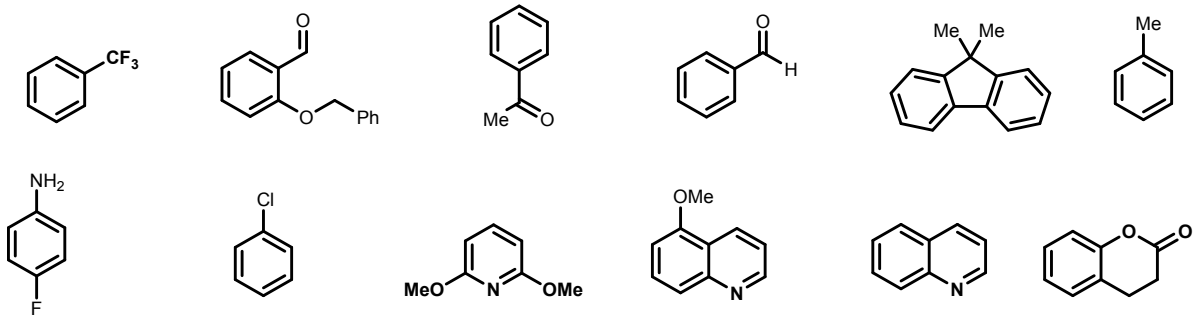

6. Cleaning procedure

Importantly: Deactivation of the electrodes occurs over time due to adsorption of organic material. Hence, this cleaning procedure needs to be strictly followed to ensure reproducibility of the electrochemical transformation.

After collecting the product, the collection vial was changed, the power supply turned off and the reactor was washed with CH_3CN (15 mL) and disassembled. First, the gasket was cleaned with acetone on both the sides. The stainless-steel electrode was first washed with 1M HCl and scrubbed with a sponge twice, then rinsed with acetone. Next, the gasket, the loops and the stainless-steel electrode were submerged in a beaker full of acetone and sonicated for 15 minutes. The graphite electrode was wiped with paper and washed with CH_3CN for 5 times. The electrode holders were washed with acetone and dried with paper. The copper contacts were first washed with 1M HCl, then scrubbed with a sponge in case of carbon deposit (anode) could be observed. Finally, they were rinsed with acetone and reassembled. Finally, all the components were dried with paper and the reactor was reassembled.

7. NMR spectra

1-mesityl-1*H*-pyrazole (1) ^{1}H NMR (400 MHz, $CDCl_3$)

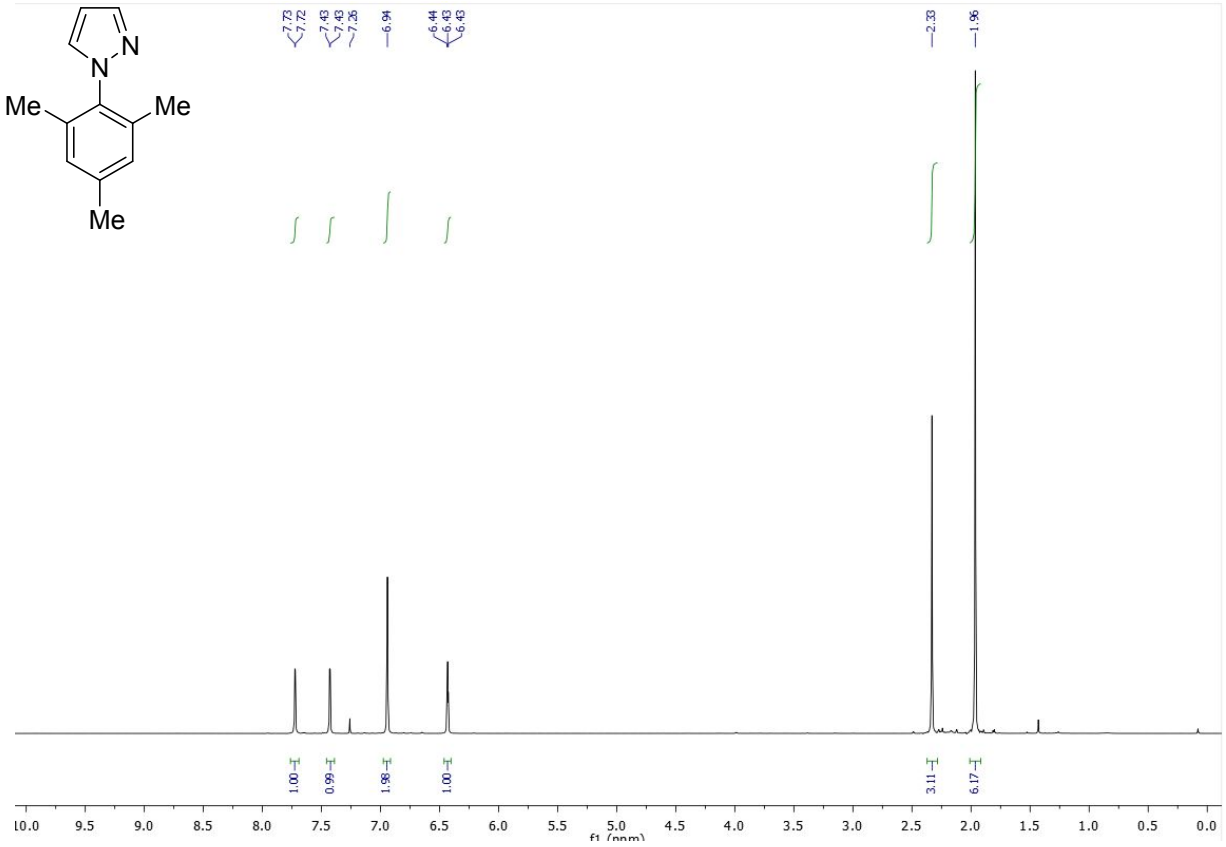

^{13}C{^{1}H} NMR (101 MHz, $CDCl_3$) (1)

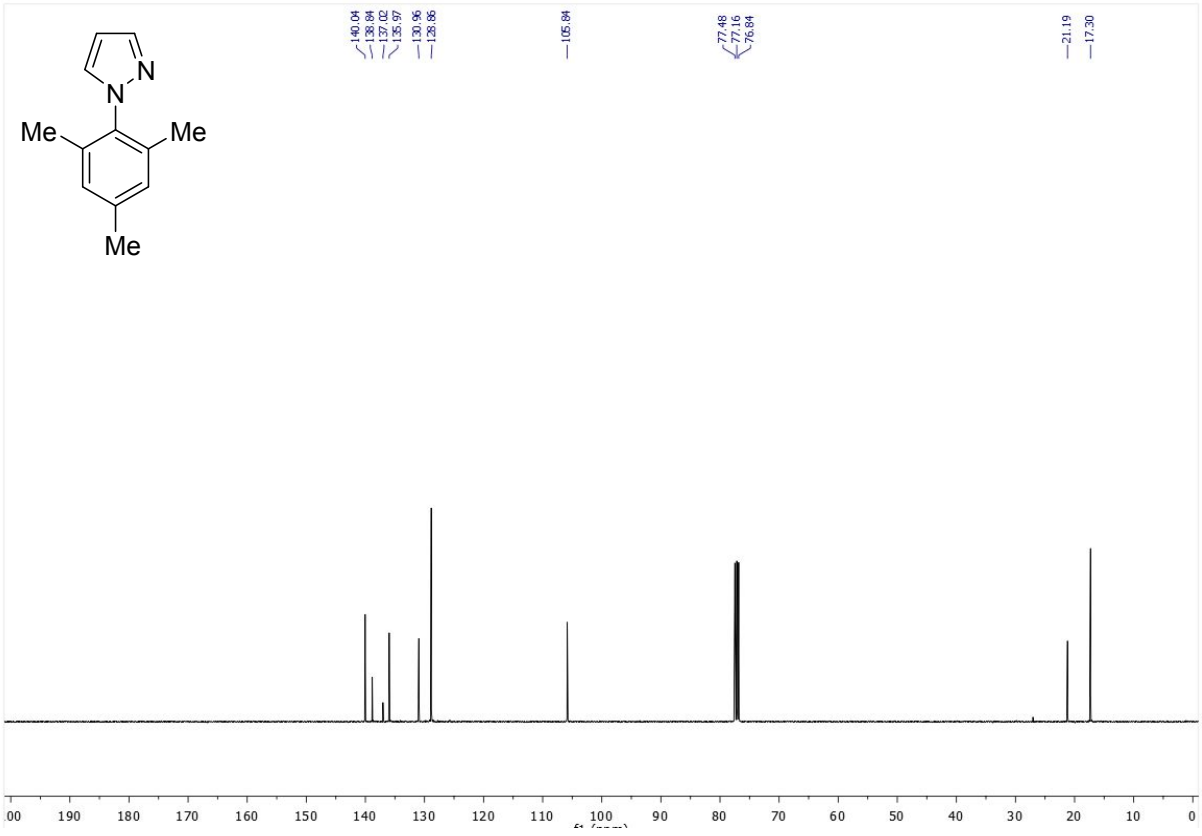

1-(naphthalen-1-yl)-1*H*-pyrazole (2) ^{1}H NMR (400 MHz, $CDCl_3$)

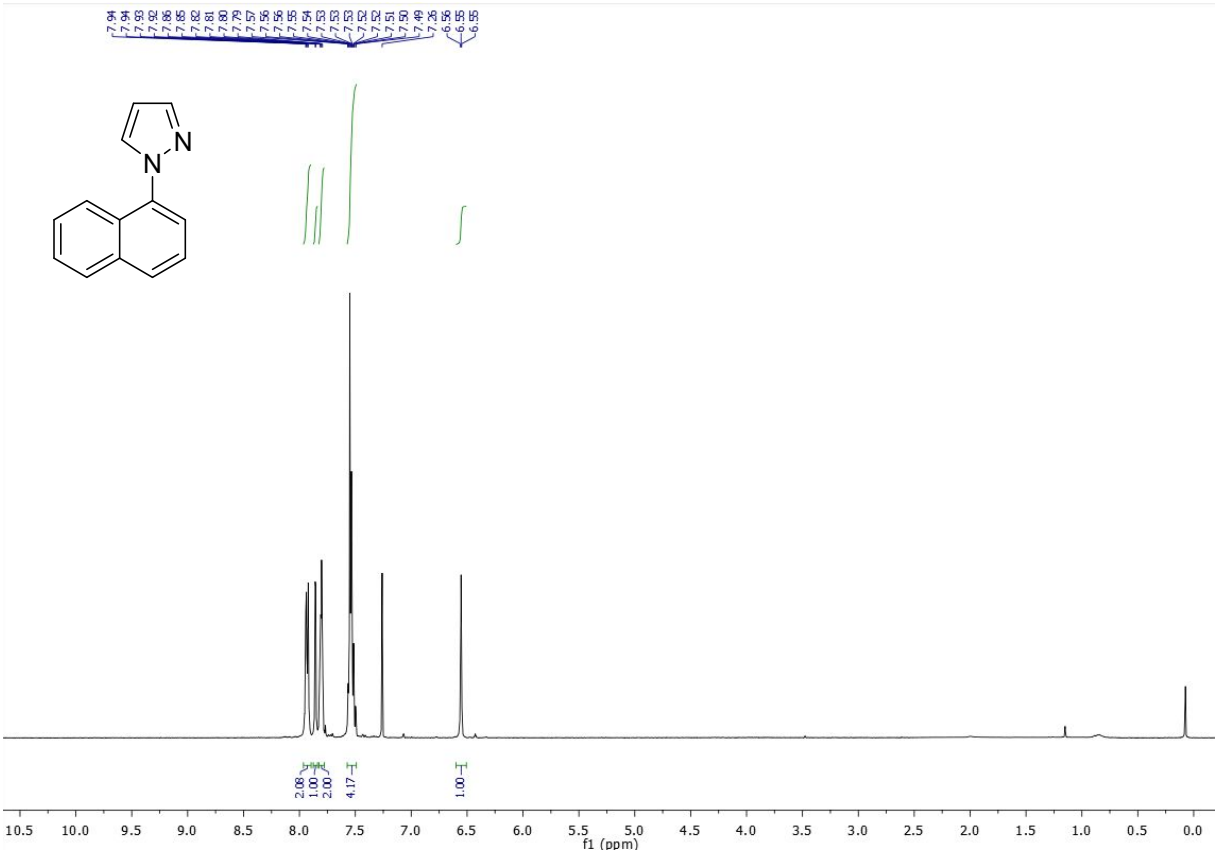

^{13}C{^{1}H} NMR (101 MHz, $CDCl_3$) (2)

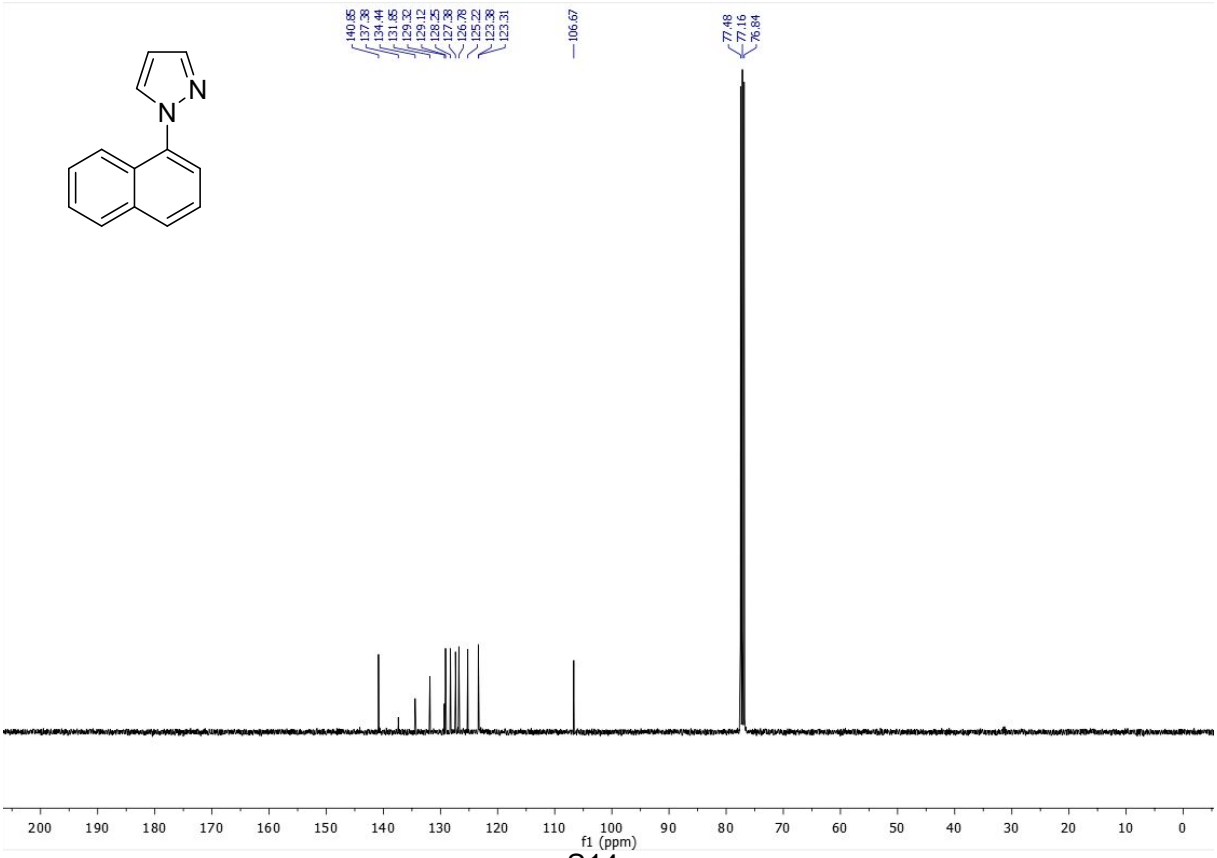

1-([1,1'-biphenyl]-4-yl)-1*H*-pyrazole (3) ^{1}H NMR (400 MHz, $CDCl_3$)

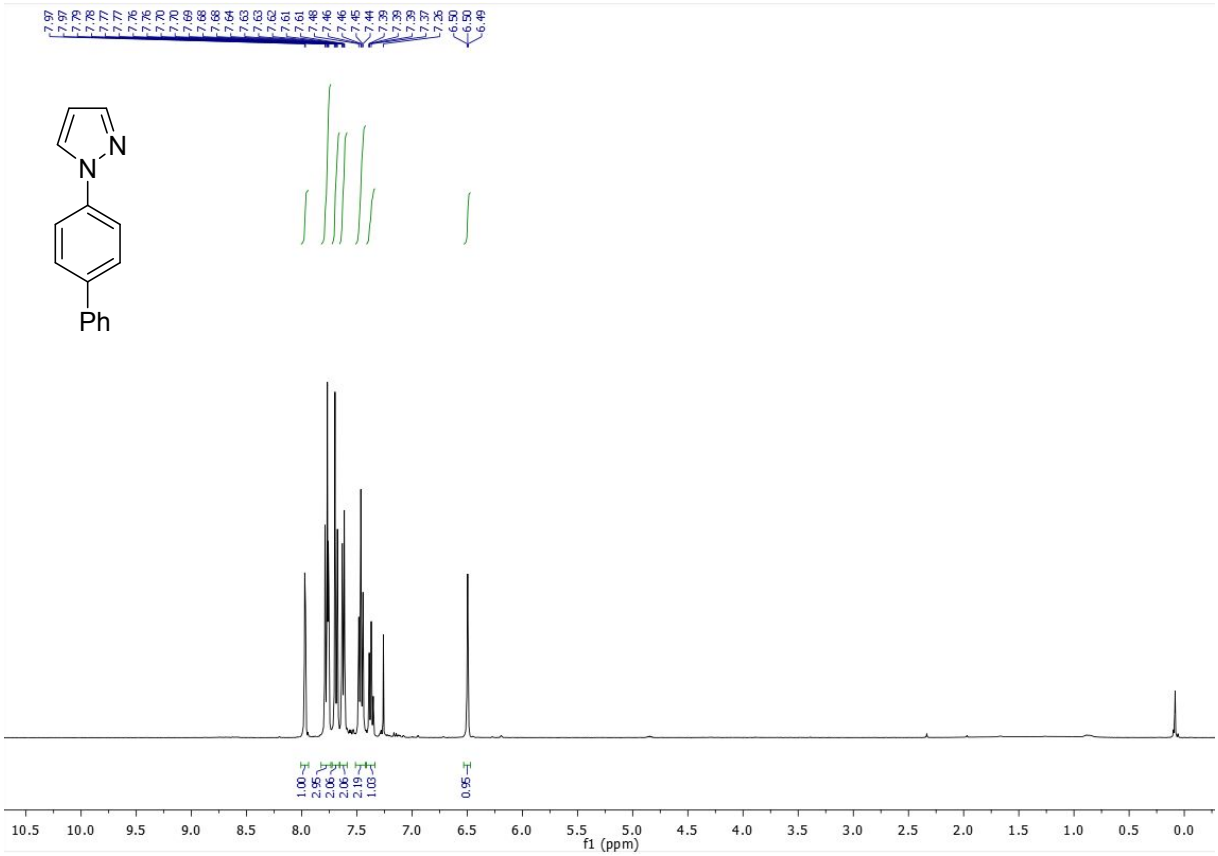

^{13}C{^{1}H} NMR (101 MHz, $CDCl_3$) (3)

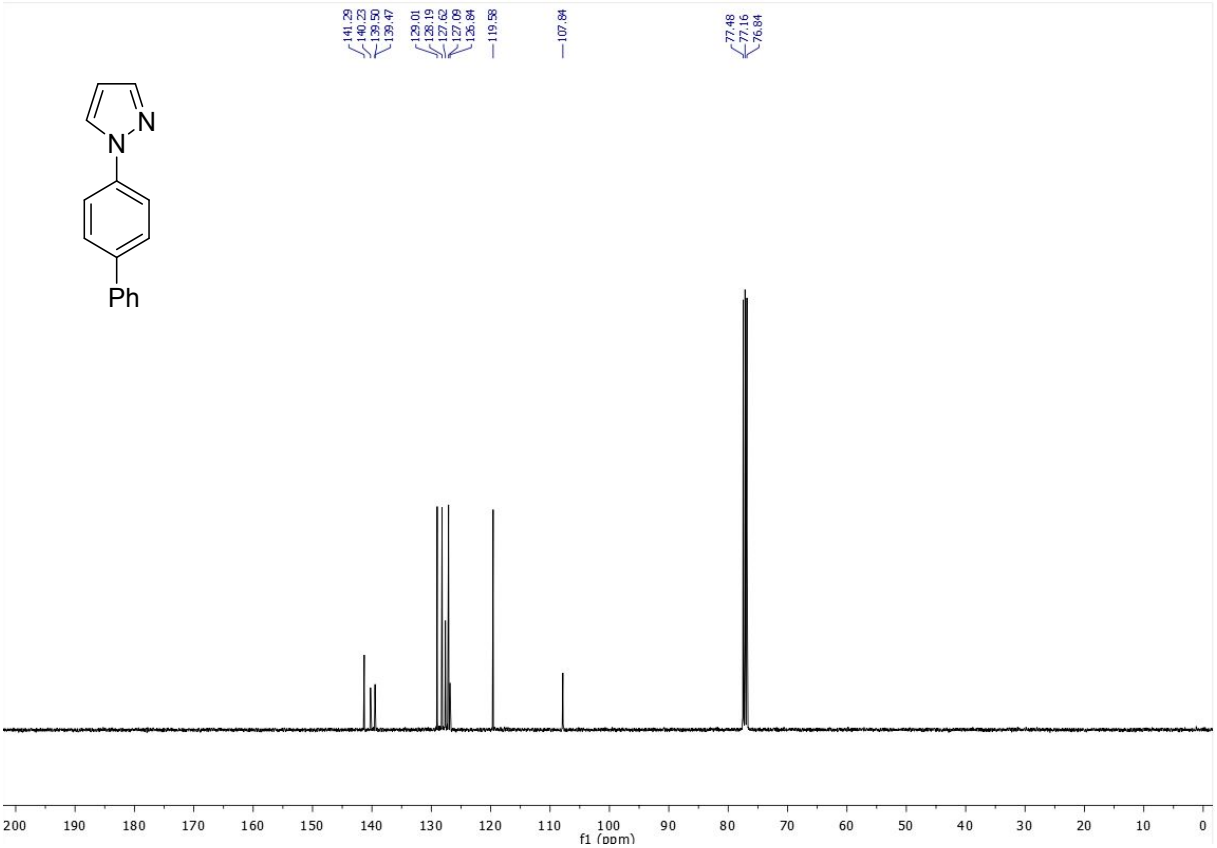

1-(2,5-di-*tert*-butylphenyl)-1*H*-pyrazole (4) ^{1}H NMR (400 MHz, $CDCl_3$)

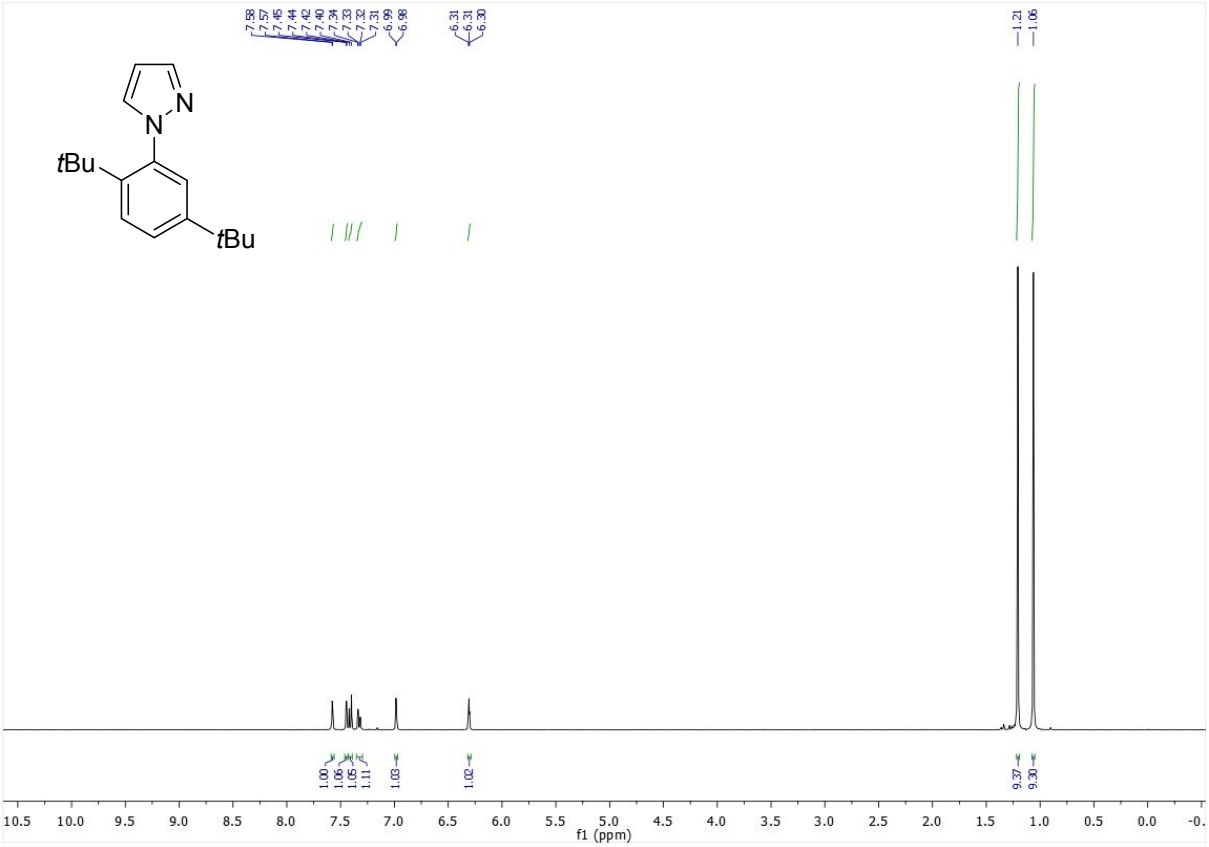

^{13}C{^{1}H} NMR (101 MHz, $CDCl_3$) (4)

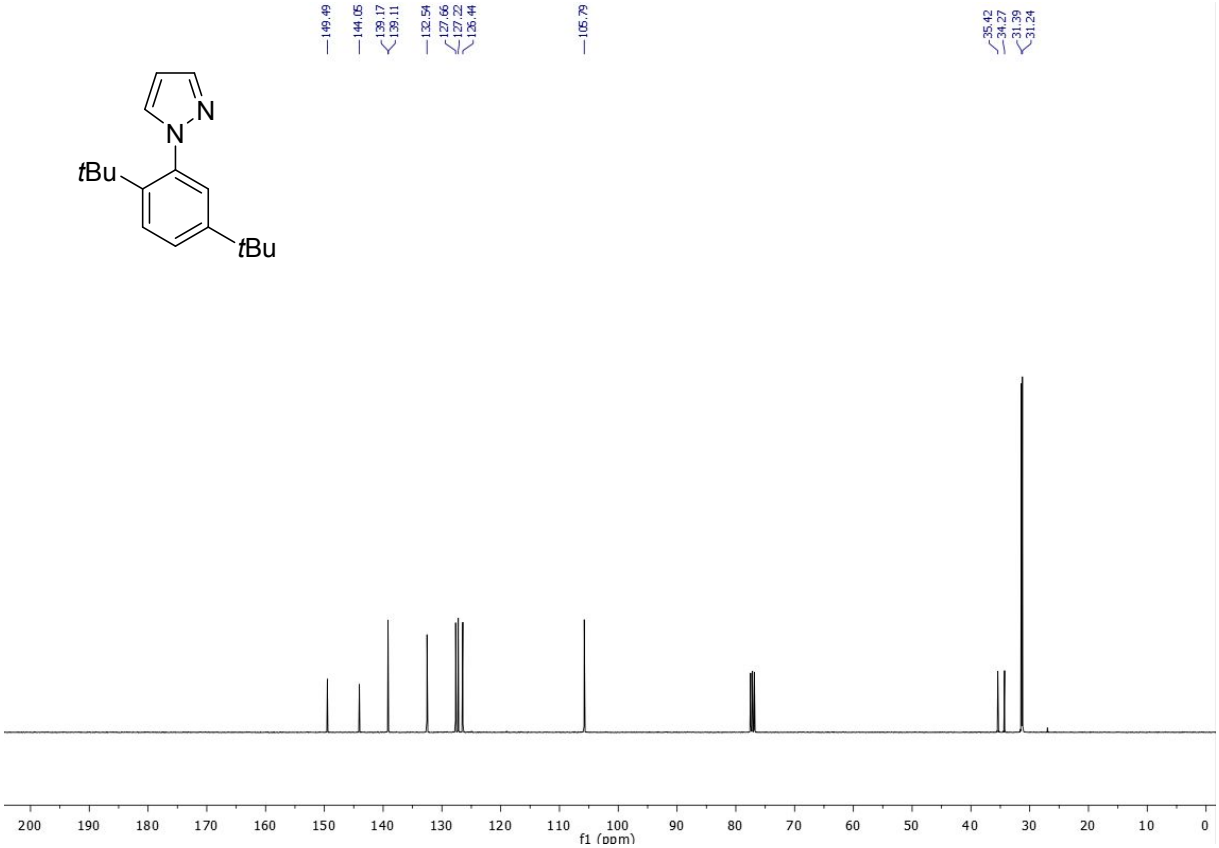

4-methoxy-2-(1*H*-pyrazol-1-yl)phenol (5) ^{1}H NMR (400 MHz, $CDCl_3$)

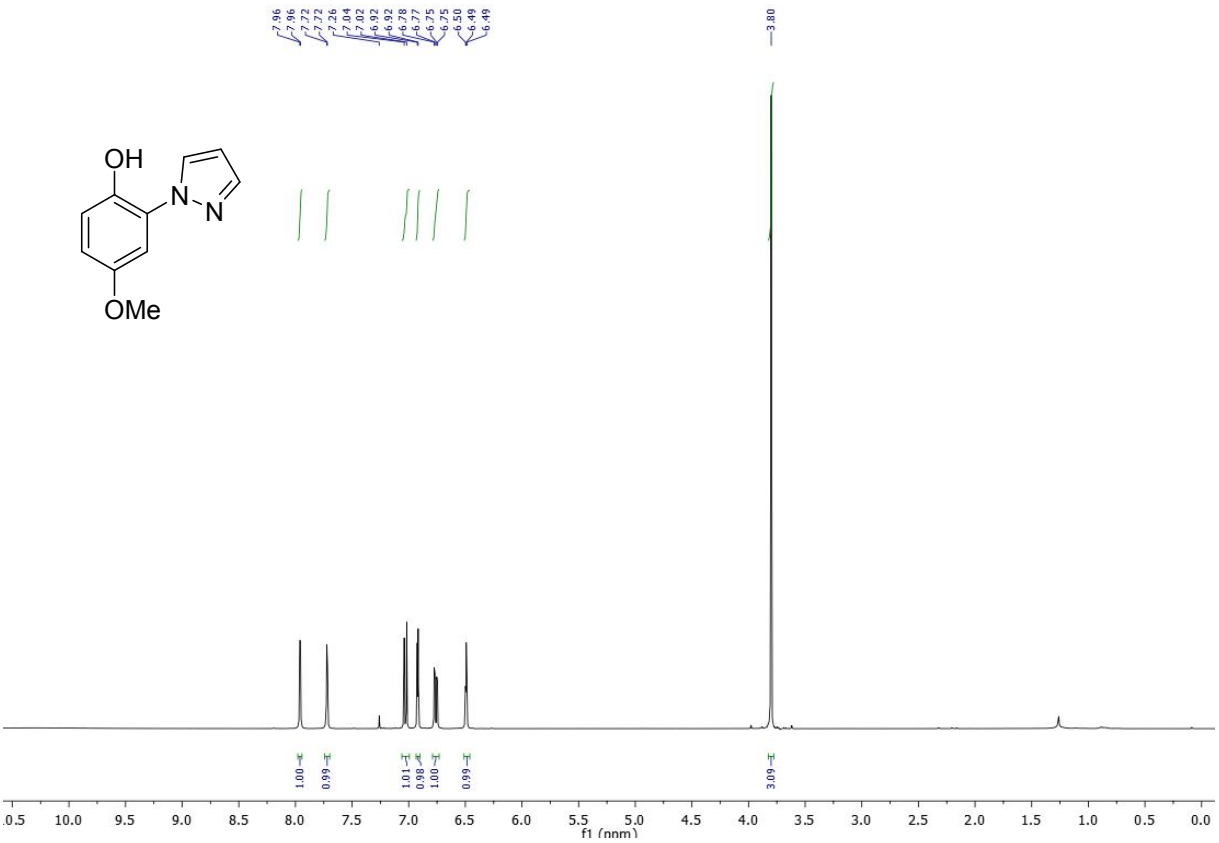

^{13}C{^{1}H} NMR (101 MHz, $CDCl_3$) (5)

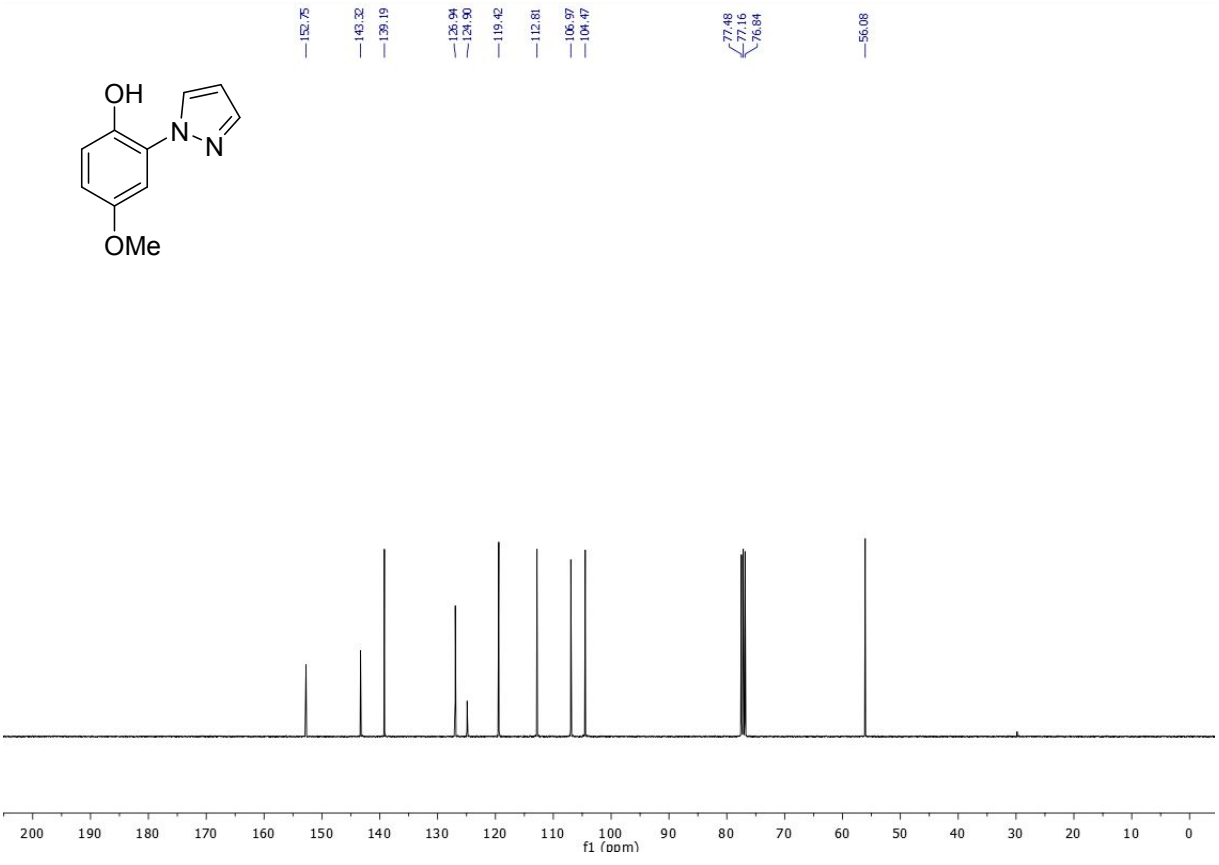

1-(2-methoxyphenyl)-1*H*-pyrazole and 1-(4-methoxyphenyl)-1*H*-pyrazole (7A and 7B)) ^{1}H NMR (400 MHz, $CDCl_3$)

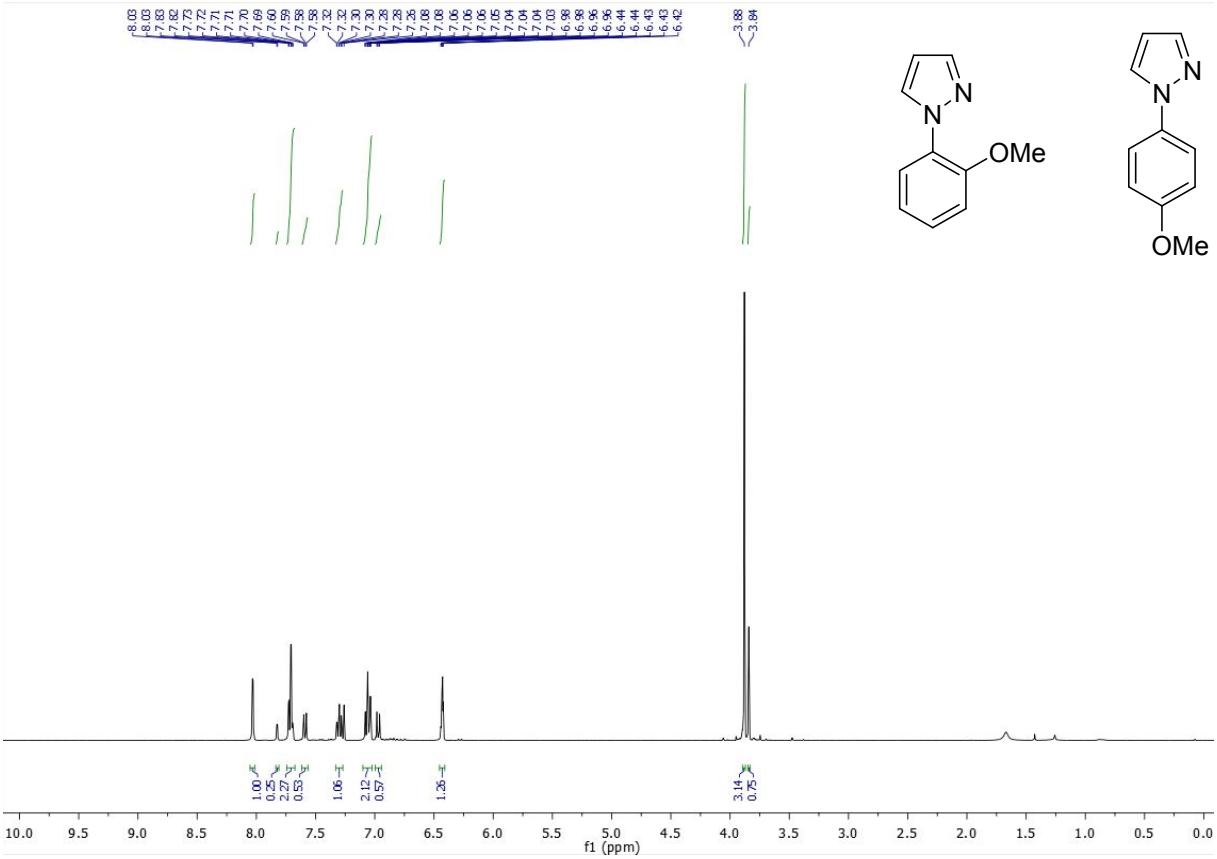

^{13}C{^{1}H} NMR (101 MHz, $CDCl_3$) (7A and 7B)

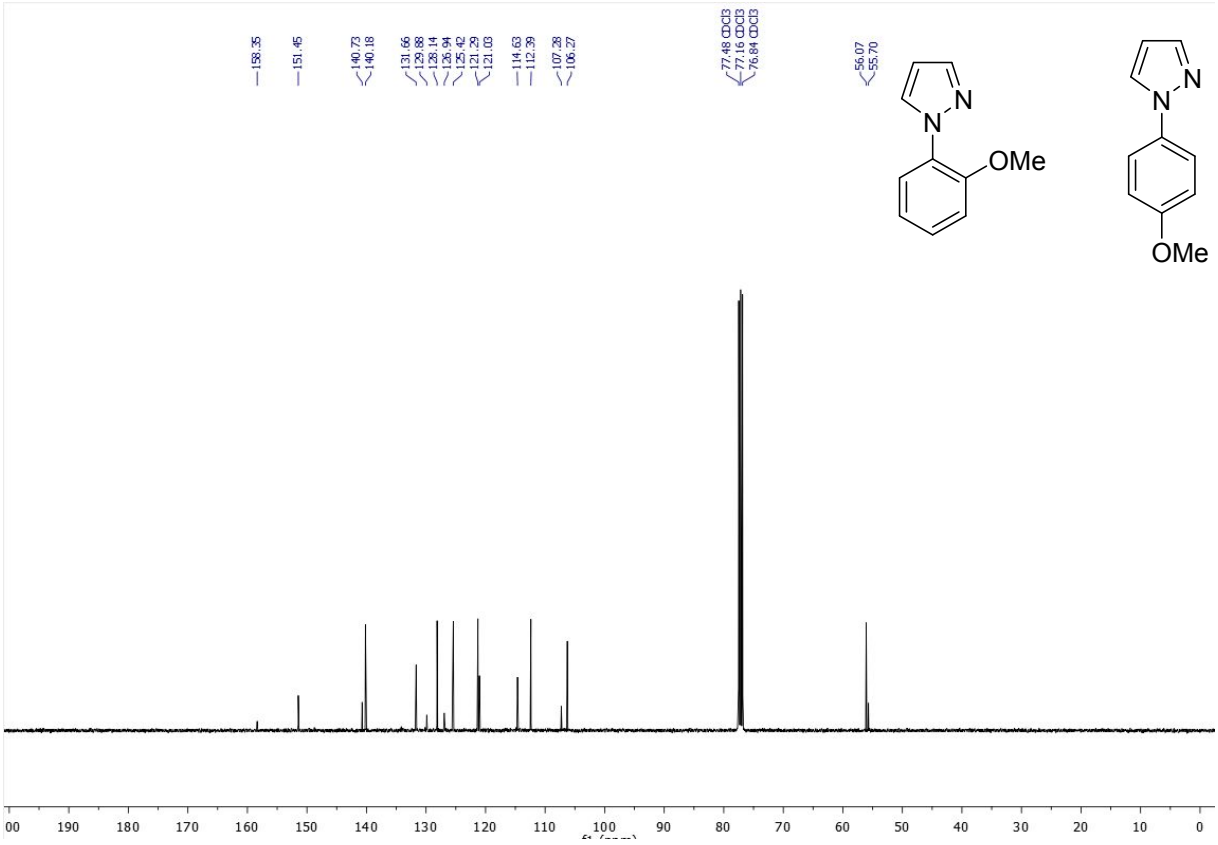

1-(2,4-dimethylphenyl)-1*H*-pyrazole (1) and 1-(2,6-dimethylphenyl)-1*H*-pyrazole (8A and 8B) ^{1}H NMR (400 MHz, $CDCl_3$)

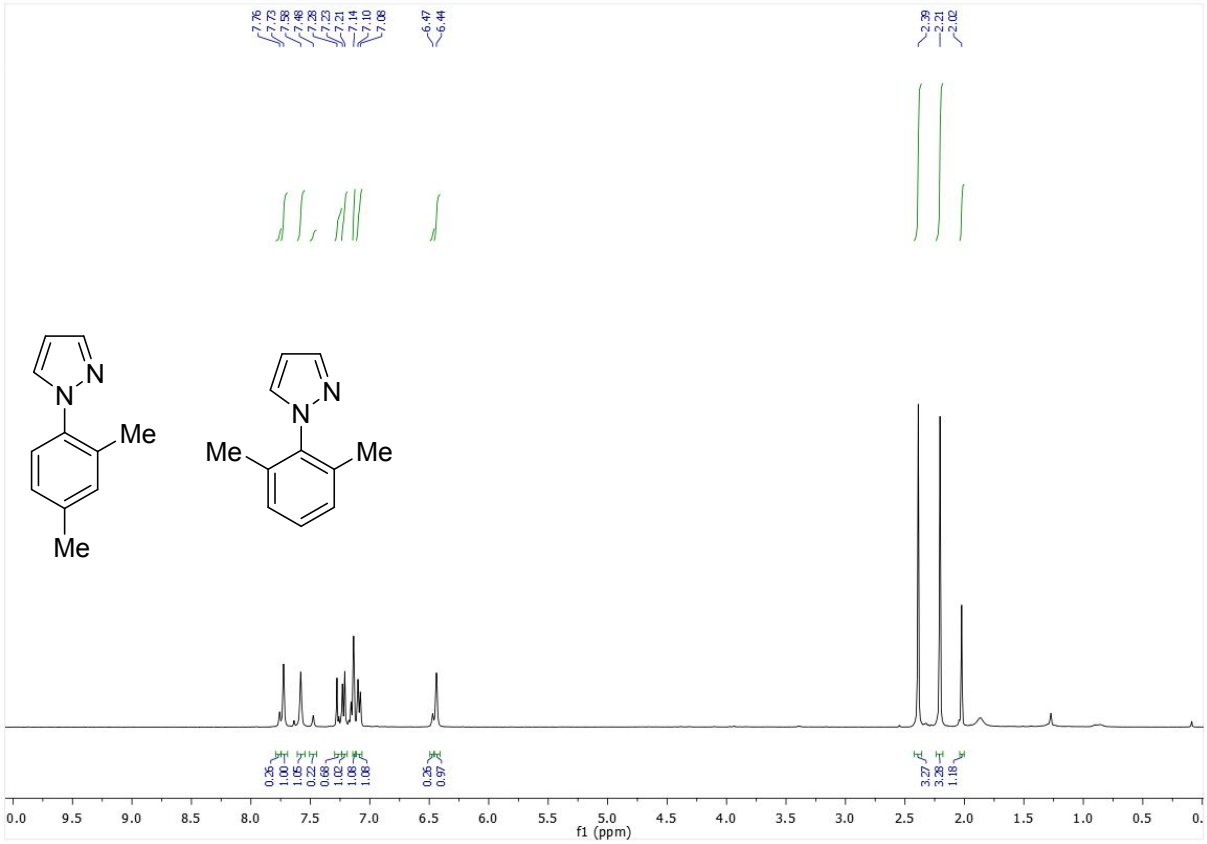

^{13}C{^{1}H} NMR (101 MHz, $CDCl_3$) (8A and 8B)

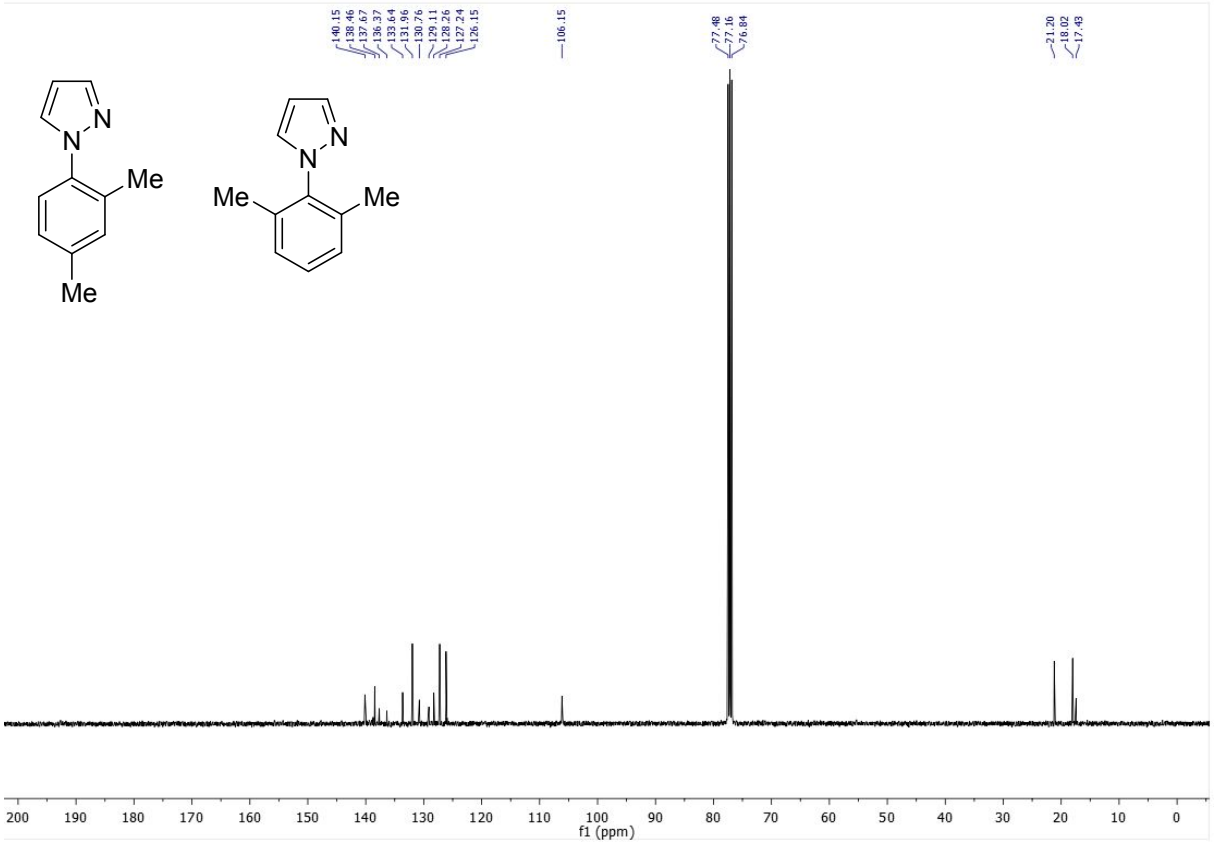

4-methoxy-3-(1*H*-pyrazol-1-yl)benzaldehyde (9) ^{1}H NMR (400 MHz, $CDCl_3$)

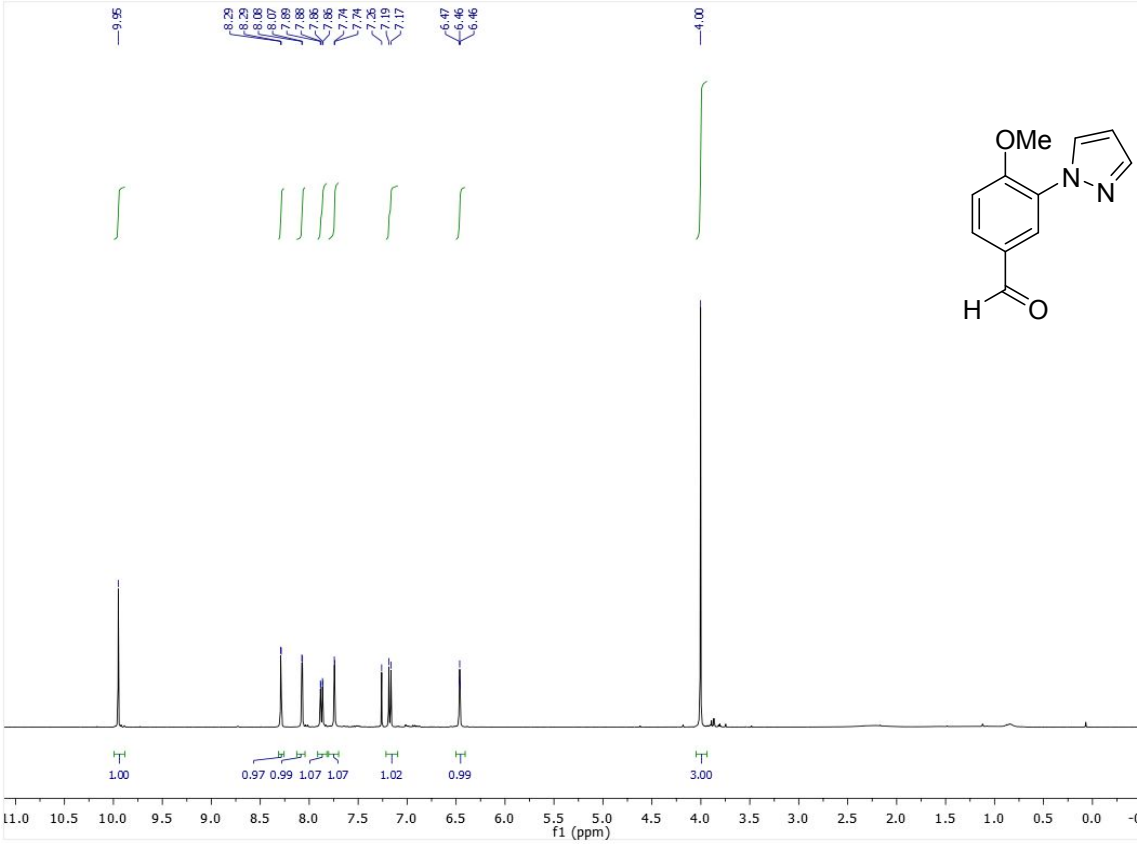

$^{13}C\{^{1}H\}$ NMR (101 MHz, $CDCl_3$) (9)

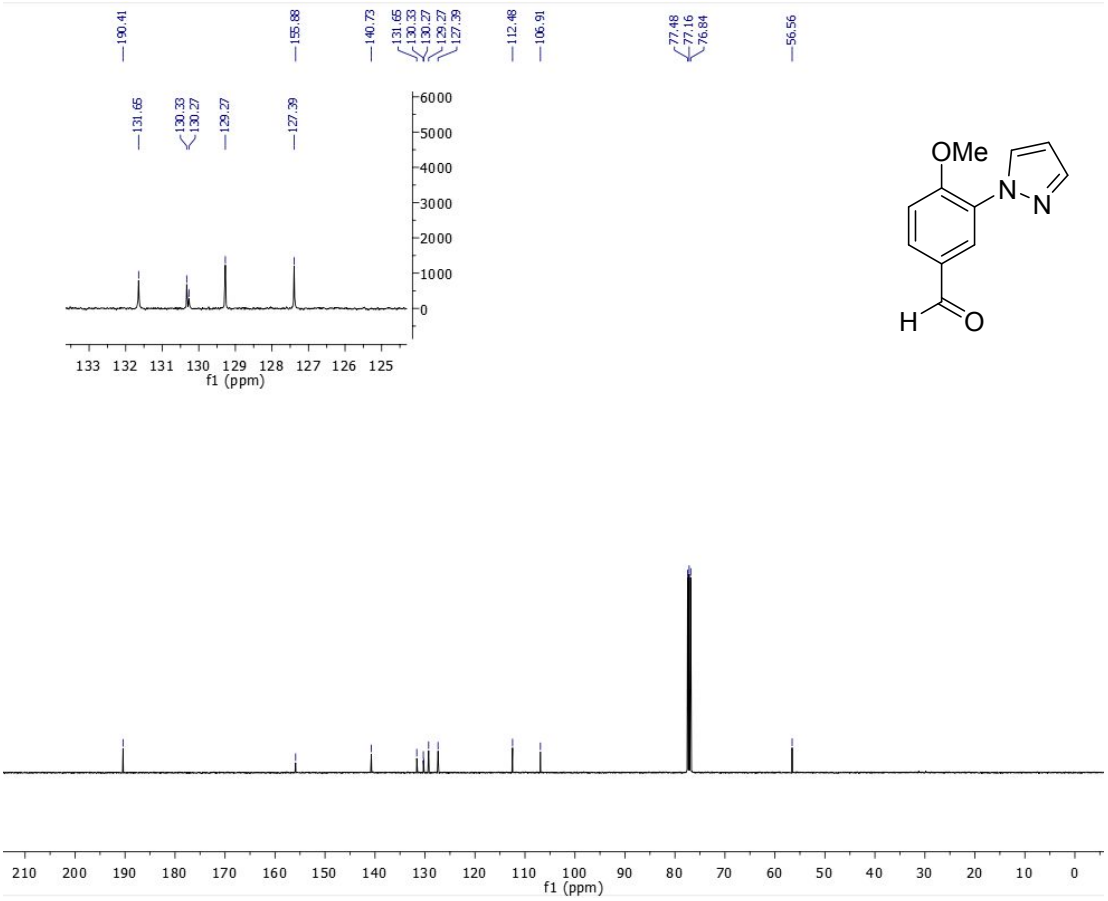

Methyl 4-methoxy-3-(1*H*-pyrazol-1-yl)benzoate (10) ^{1}H NMR (400 MHz, $CDCl_3$)

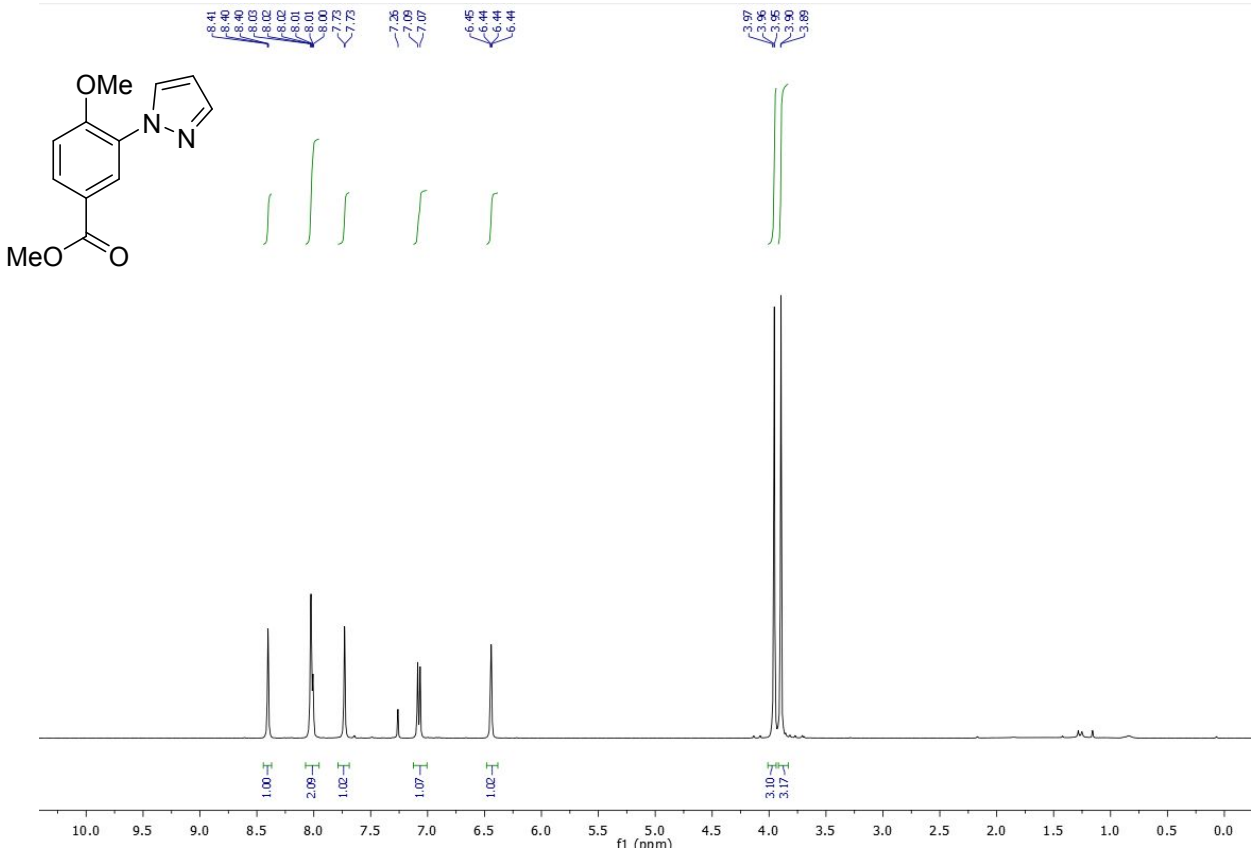

$^{13}C\{^{1}H\}$ NMR (101 MHz, $CDCl_3$) (10)

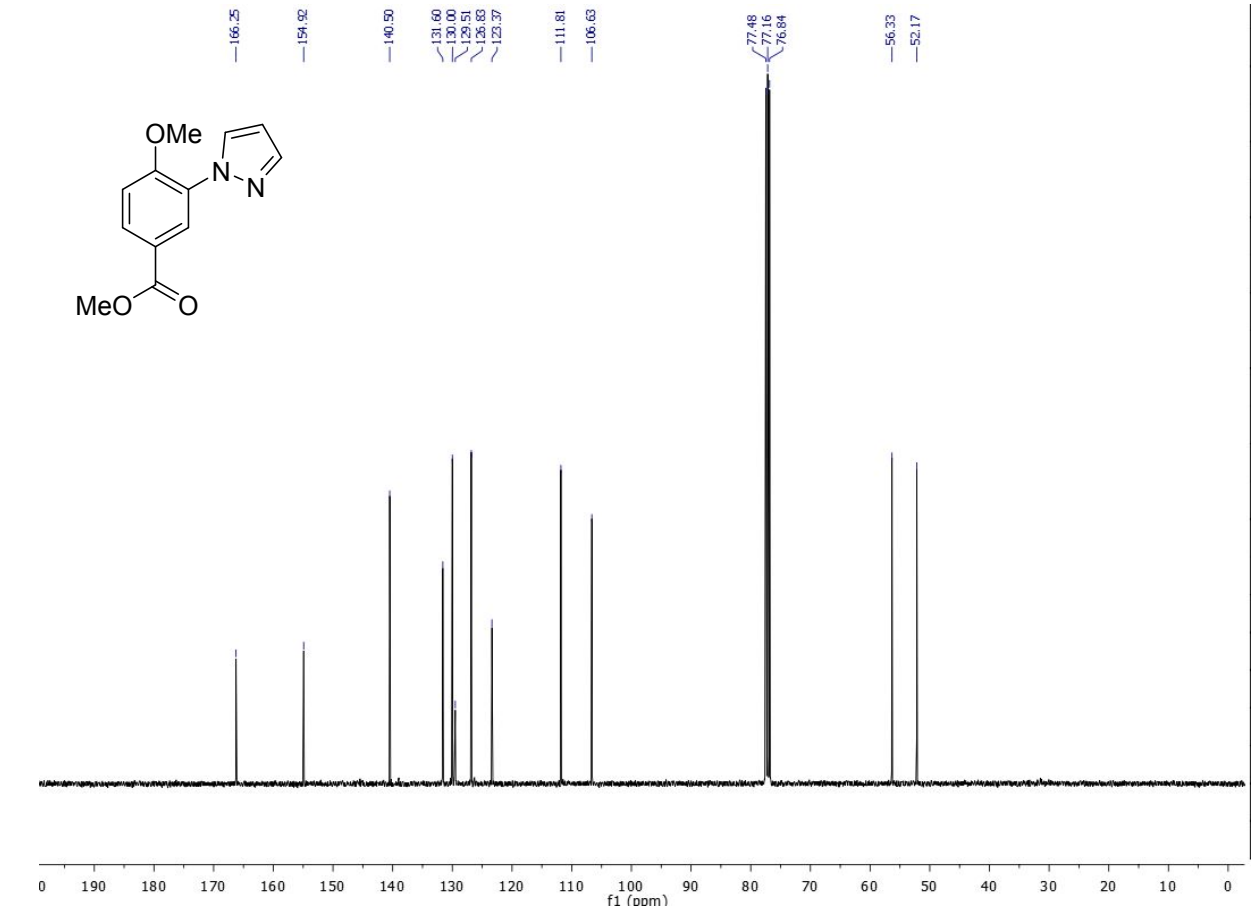

1-(4-methoxy-3-(1*H*-pyrazol-1-yl)phenyl)ethan-1-one (11) ^{1}H NMR (400 MHz, $CDCl_3$)

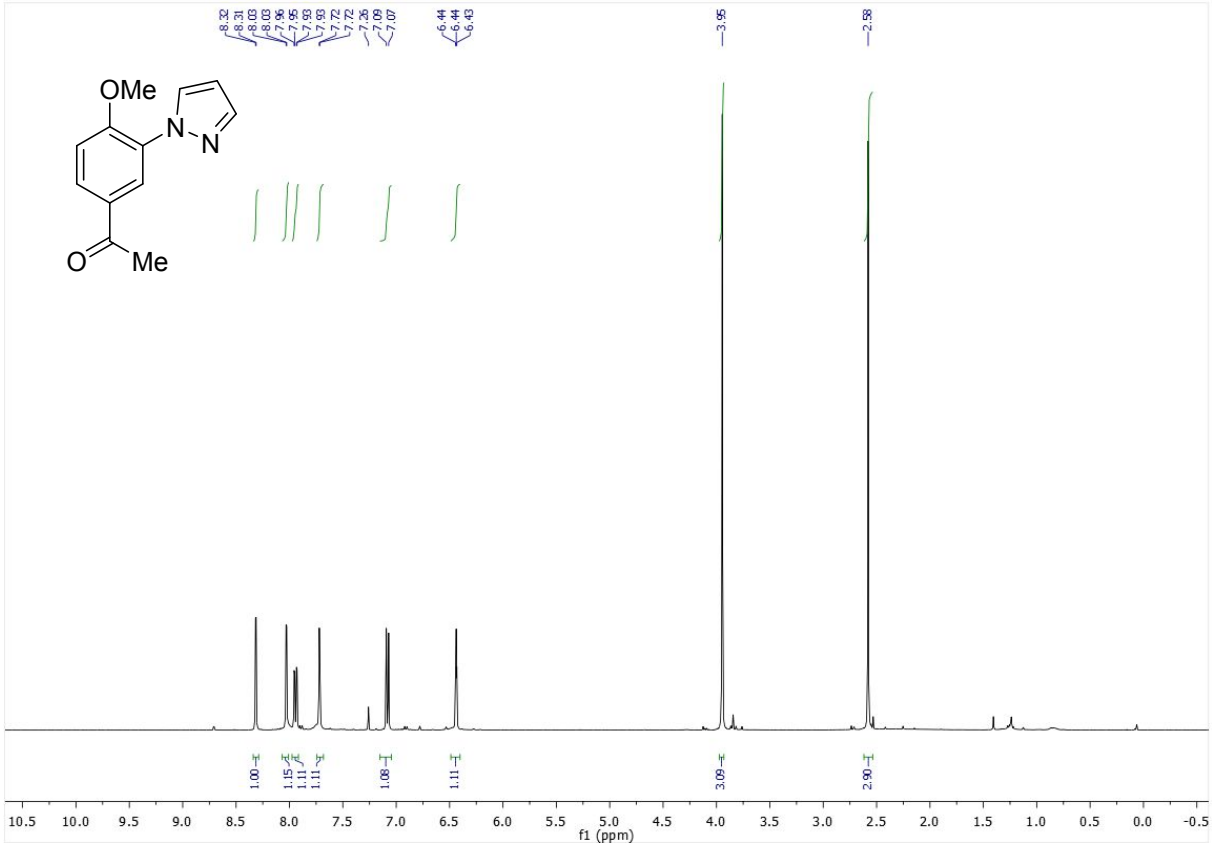

^{13}C{^{1}H} NMR (101 MHz, $CDCl_3$) (11)

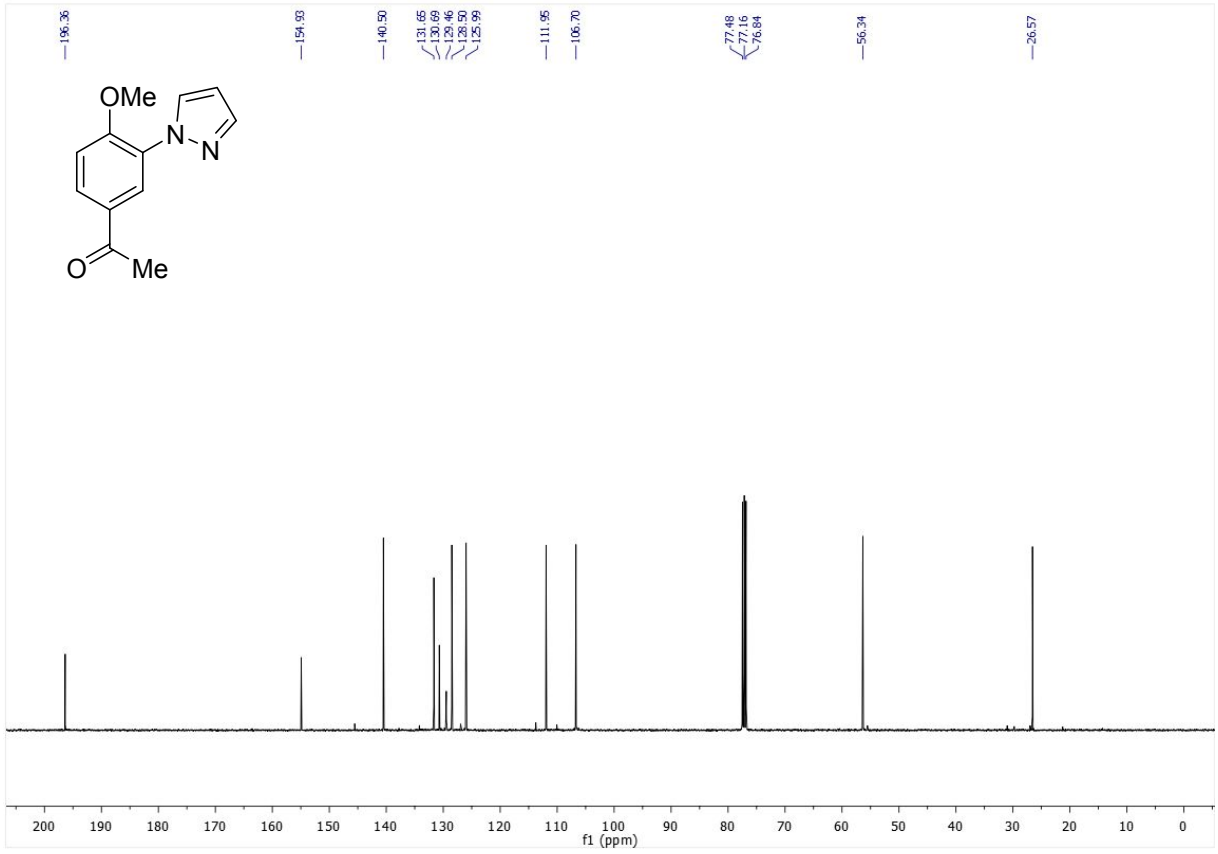

N-(4-methoxy-3-(1*H*-pyrazol-1-yl)phenyl)acetamide (12) ^{1}H NMR (400 MHz, $CDCl_3$)

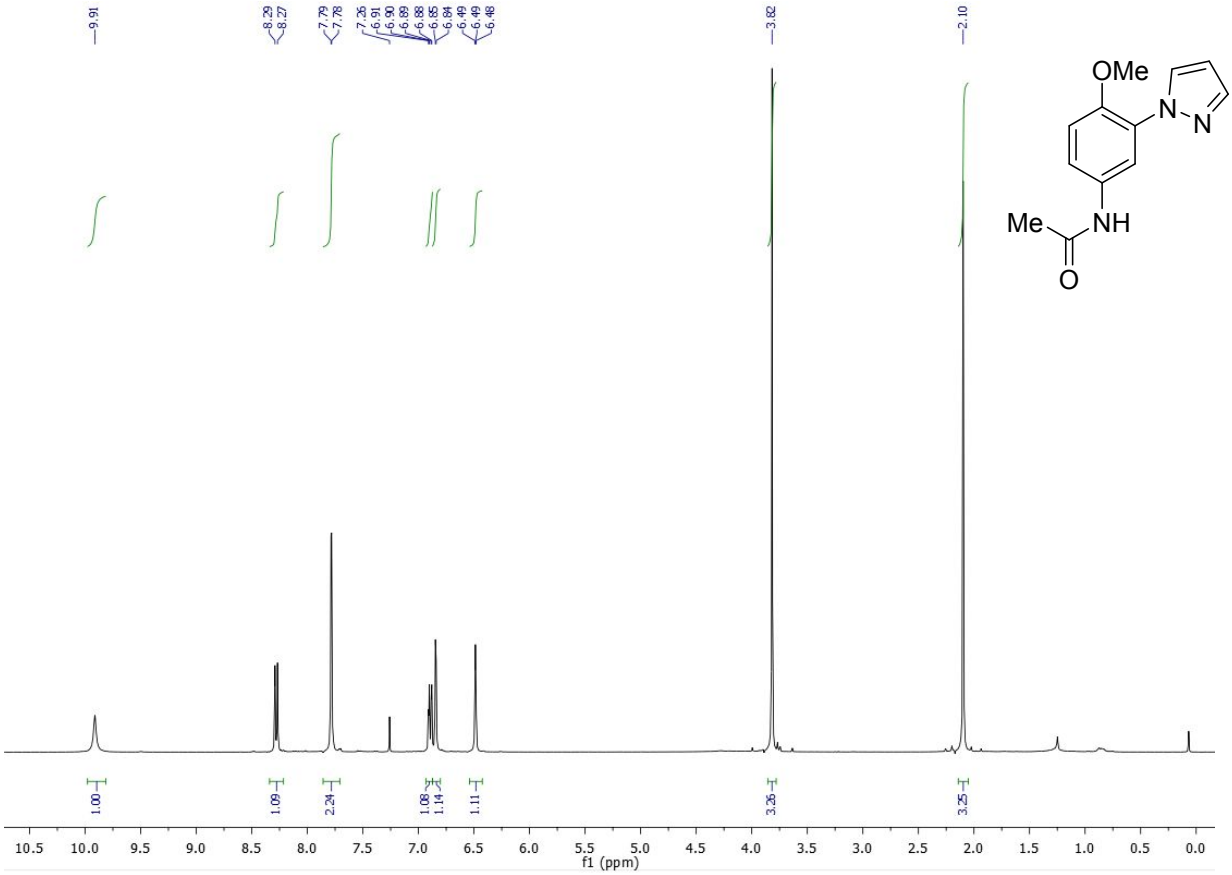

^{13}C{^{1}H} NMR (101 MHz, $CDCl_3$) (12)

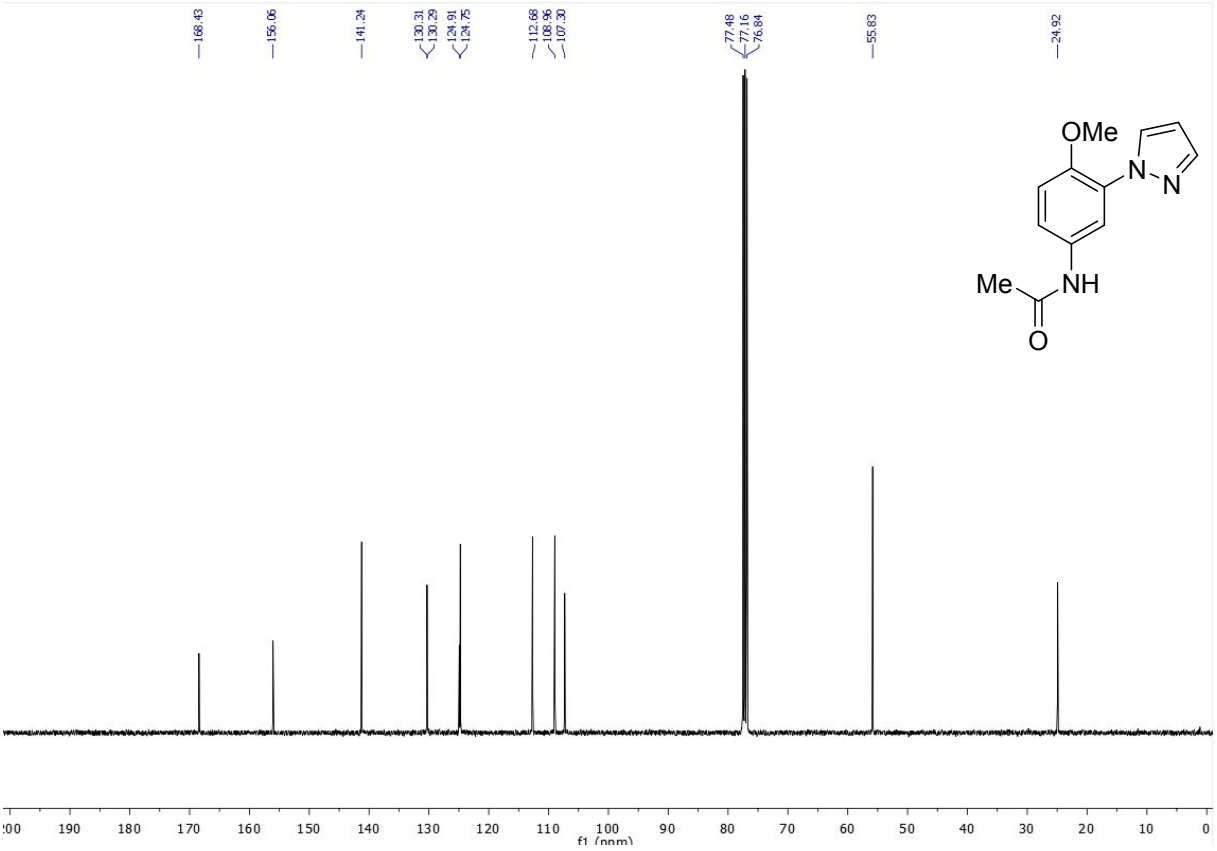

1-mesityl-4-methyl-1*H*-pyrazole (14) ^{1}H NMR (400 MHz, $CDCl_3$)

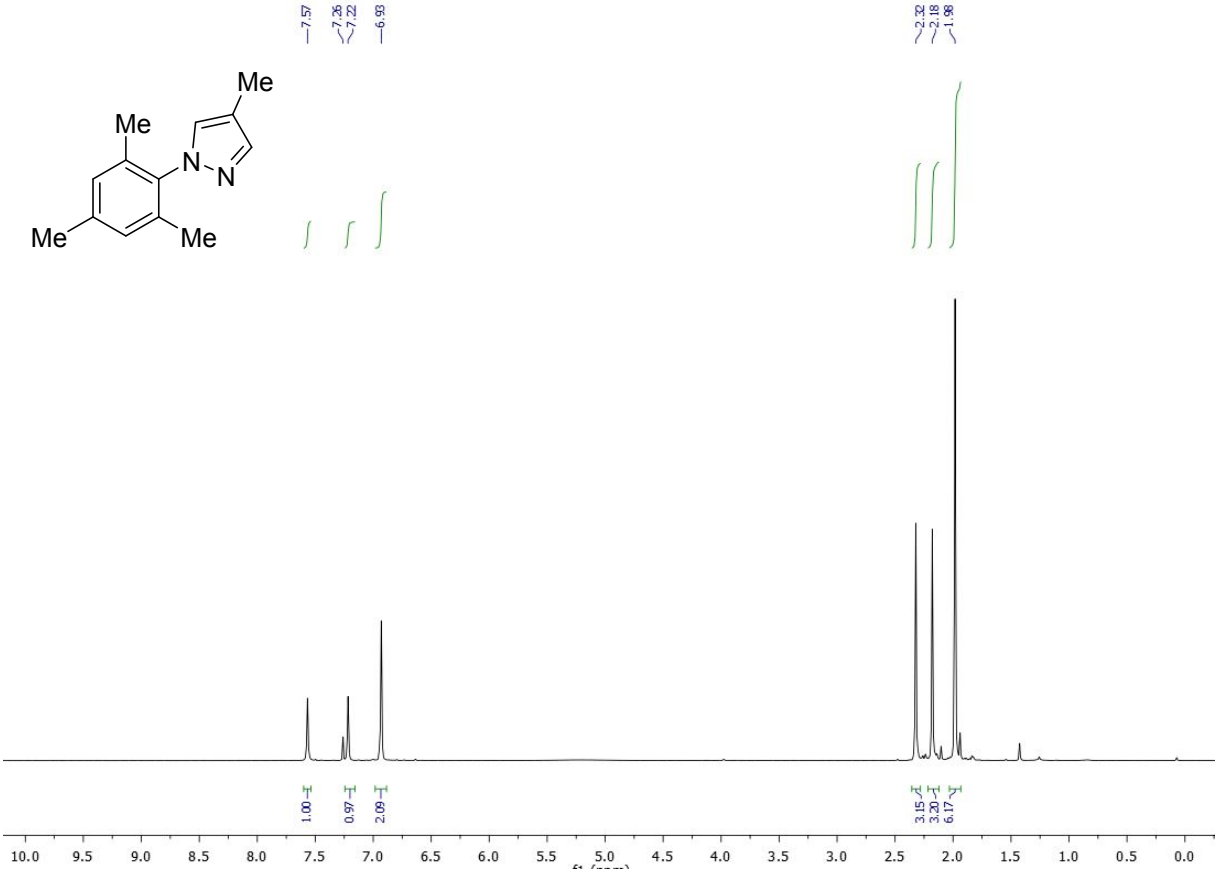

^{13}C{^{1}H} NMR (101 MHz, $CDCl_3$) (14)

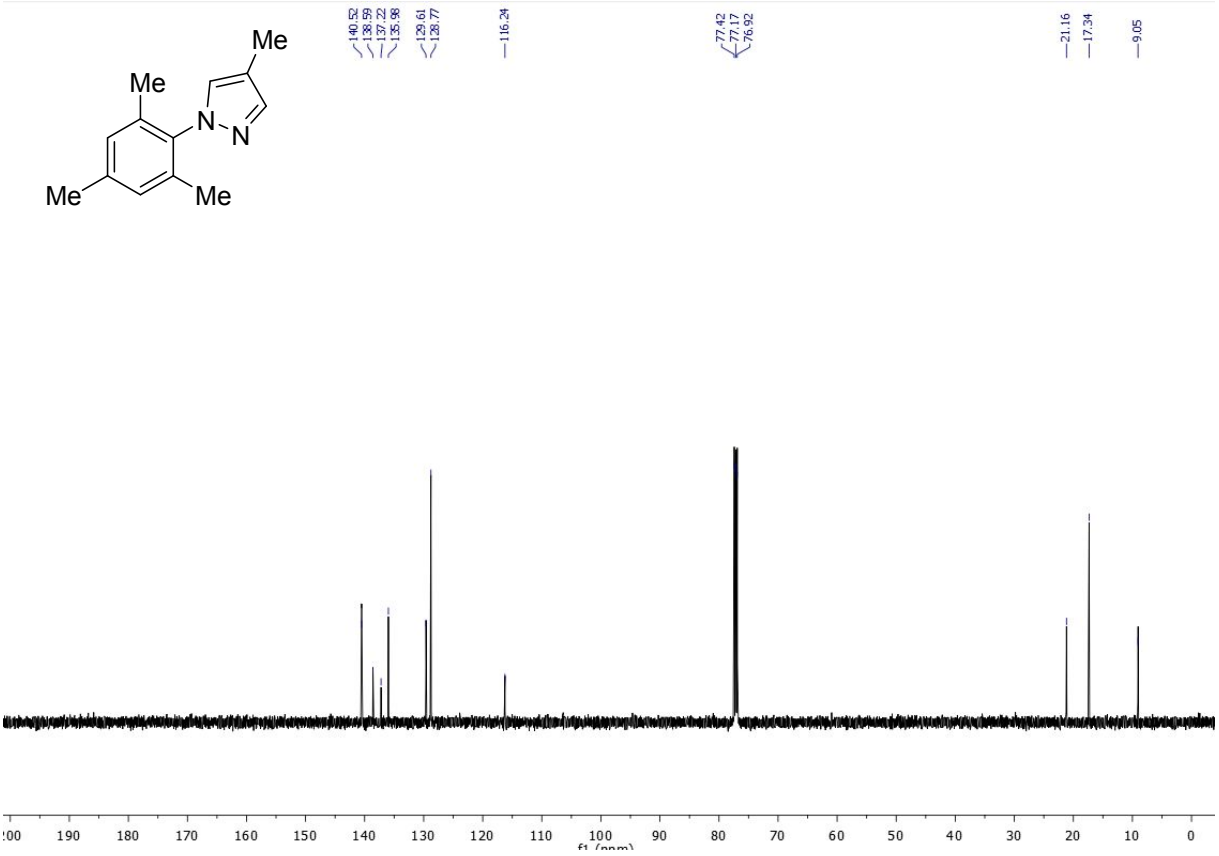

1-mesityl-3,5-dimethyl-1*H*-pyrazole (15) ^{1}H NMR (400 MHz, $CDCl_3$)

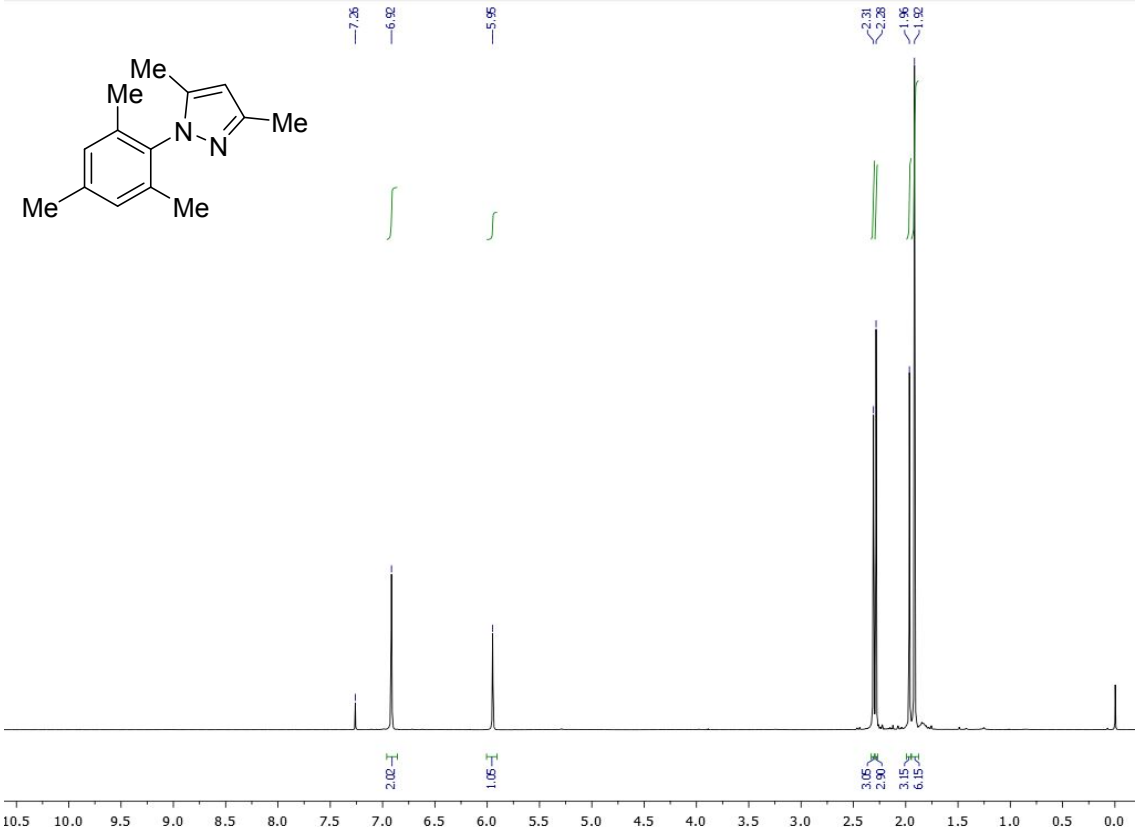

^{13}C{^{1}H} NMR (101 MHz, $CDCl_3$) (15)

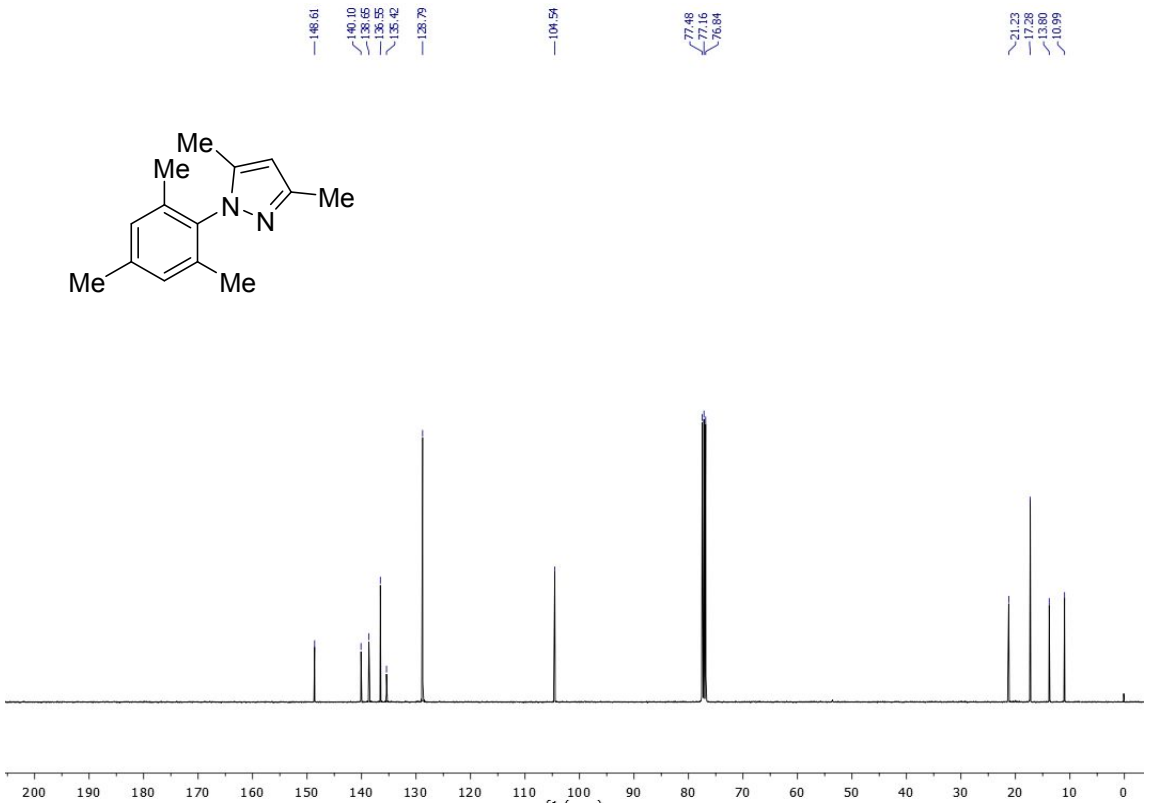

4-chloro-1-mesityl-1*H*-pyrazole (16) ^{1}H NMR (400 MHz, $CDCl_3$)

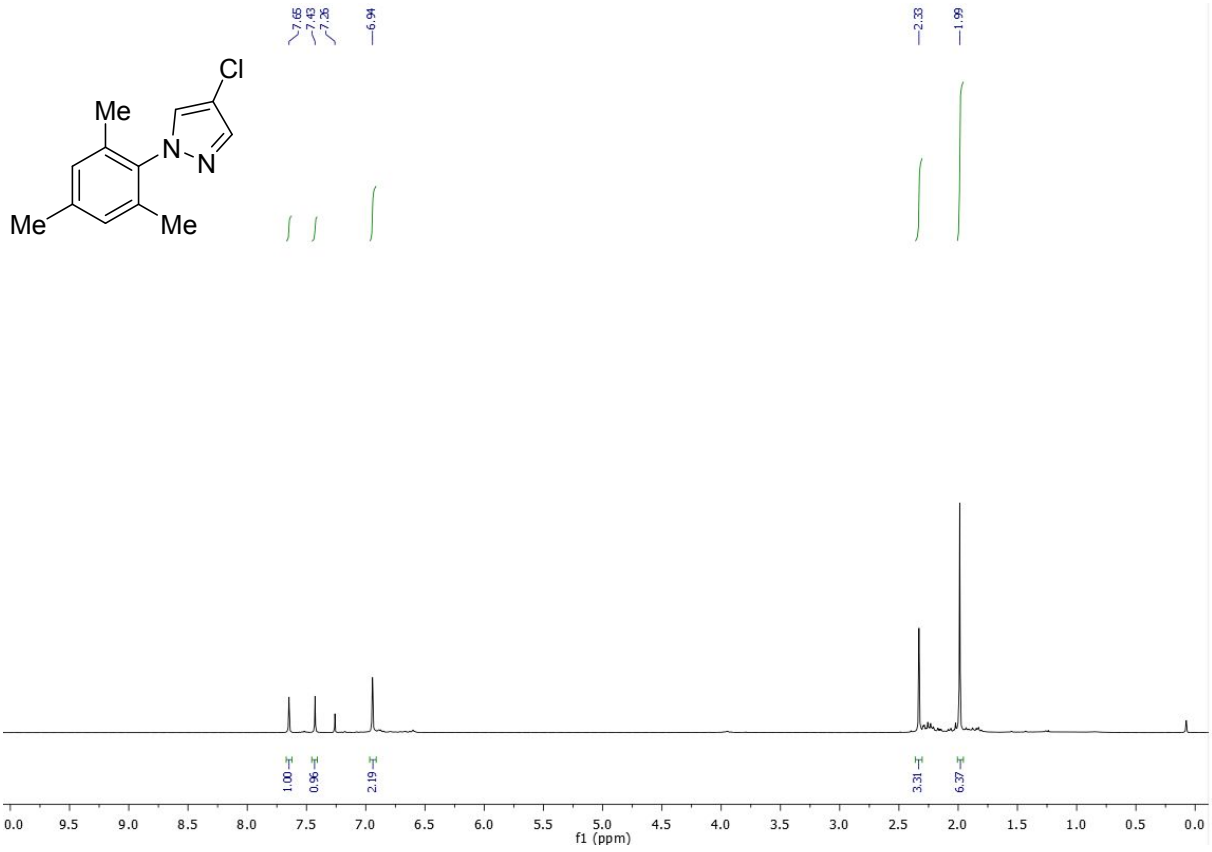

^{13}C{^{1}H} NMR (101 MHz, $CDCl_3$) (16)

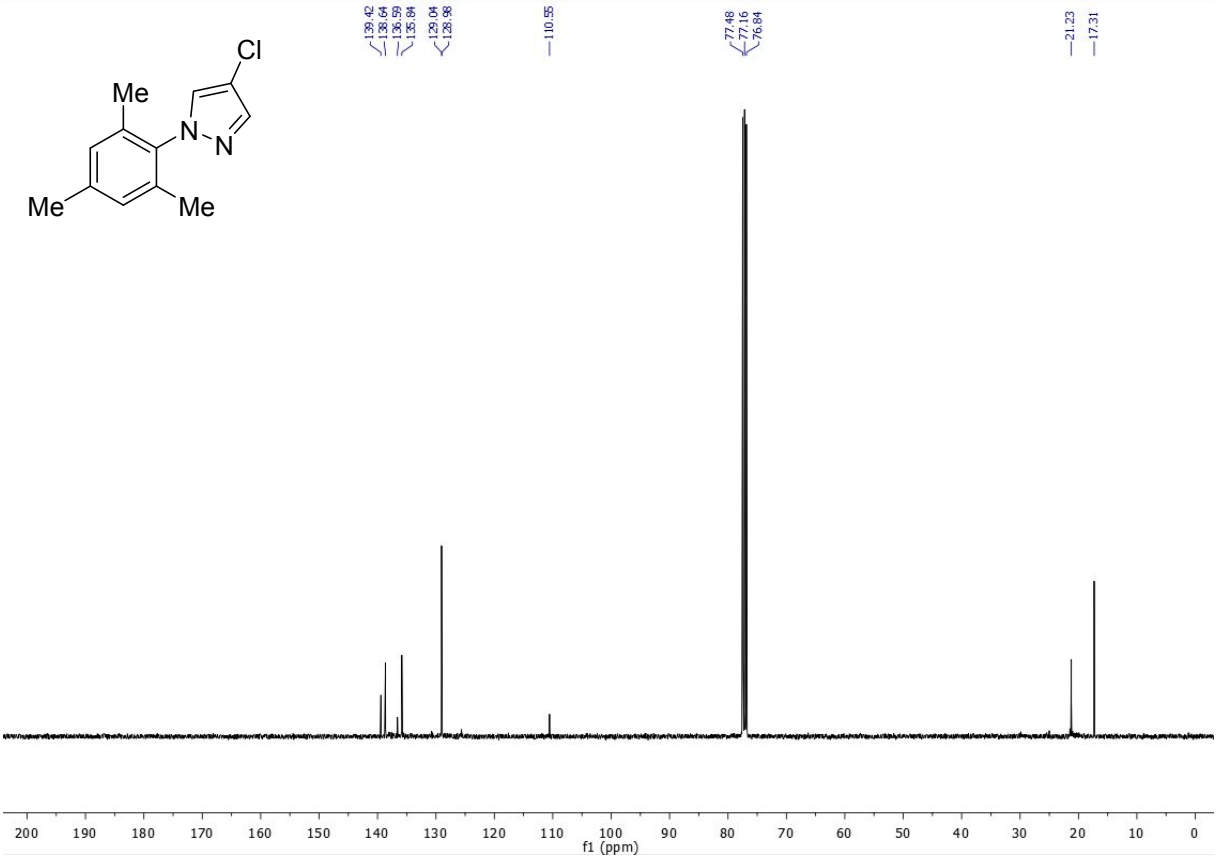

4-bromo-1-mesityl-1*H*-pyrazole (17) ^{1}H NMR (400 MHz, $CDCl_3$)

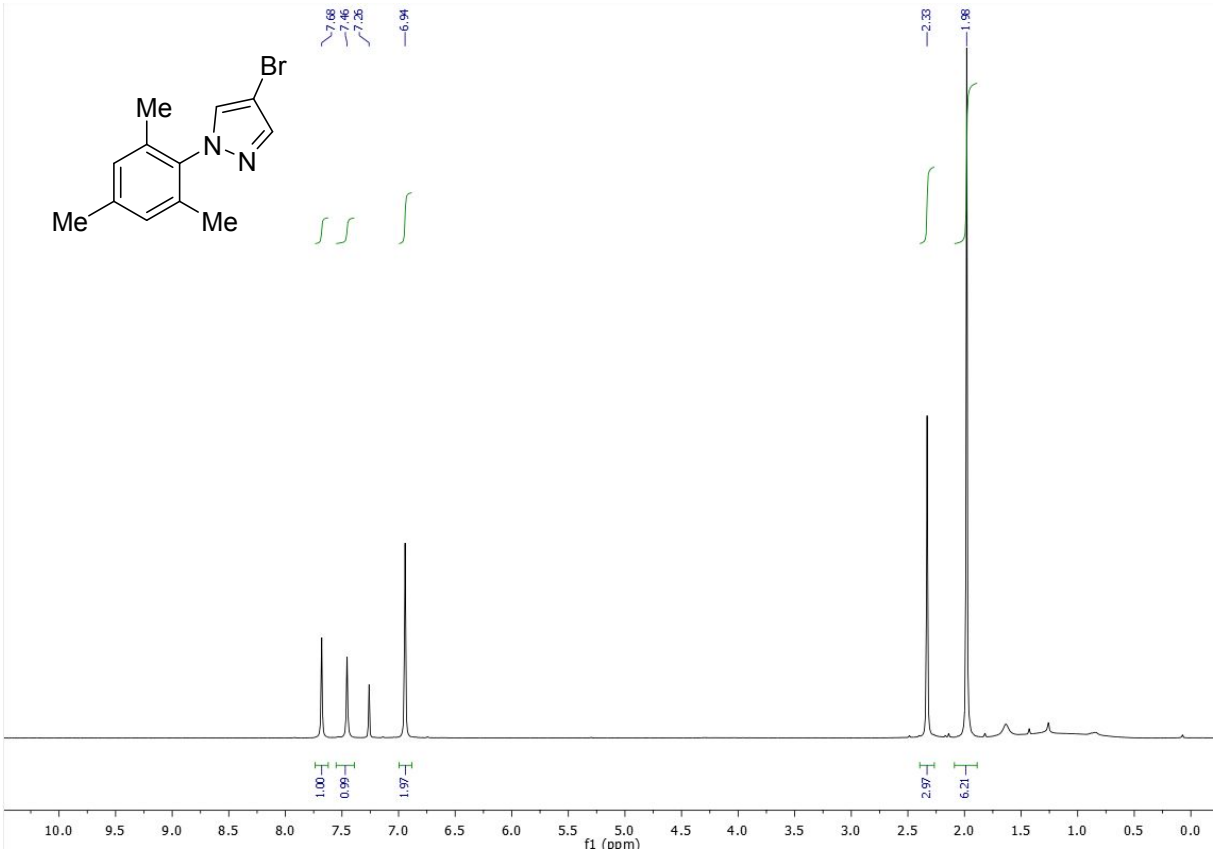

^{13}C{^{1}H} NMR (101 MHz, $CDCl_3$) (17)

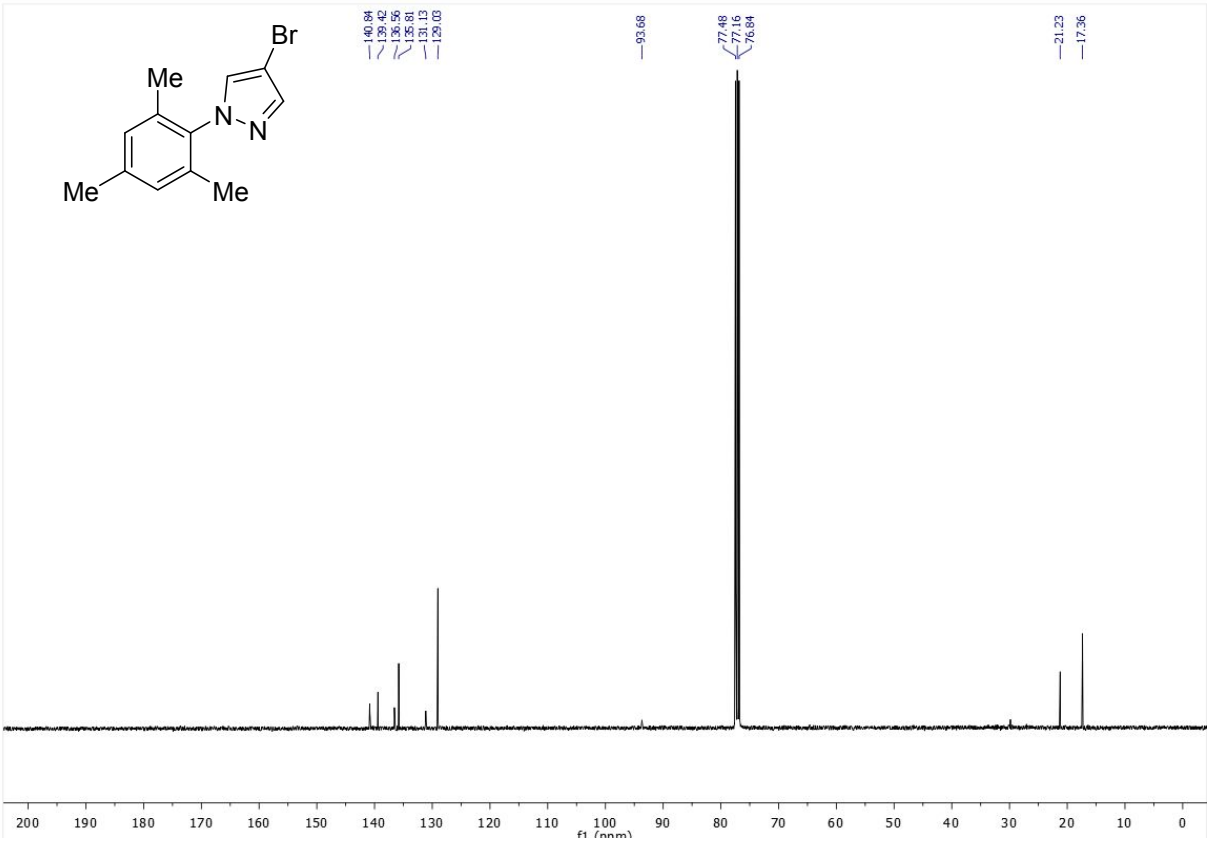

1-mesityl-1*H*-1,2,4-triazole (18) ^{1}H NMR (400 MHz, $CDCl_3$)

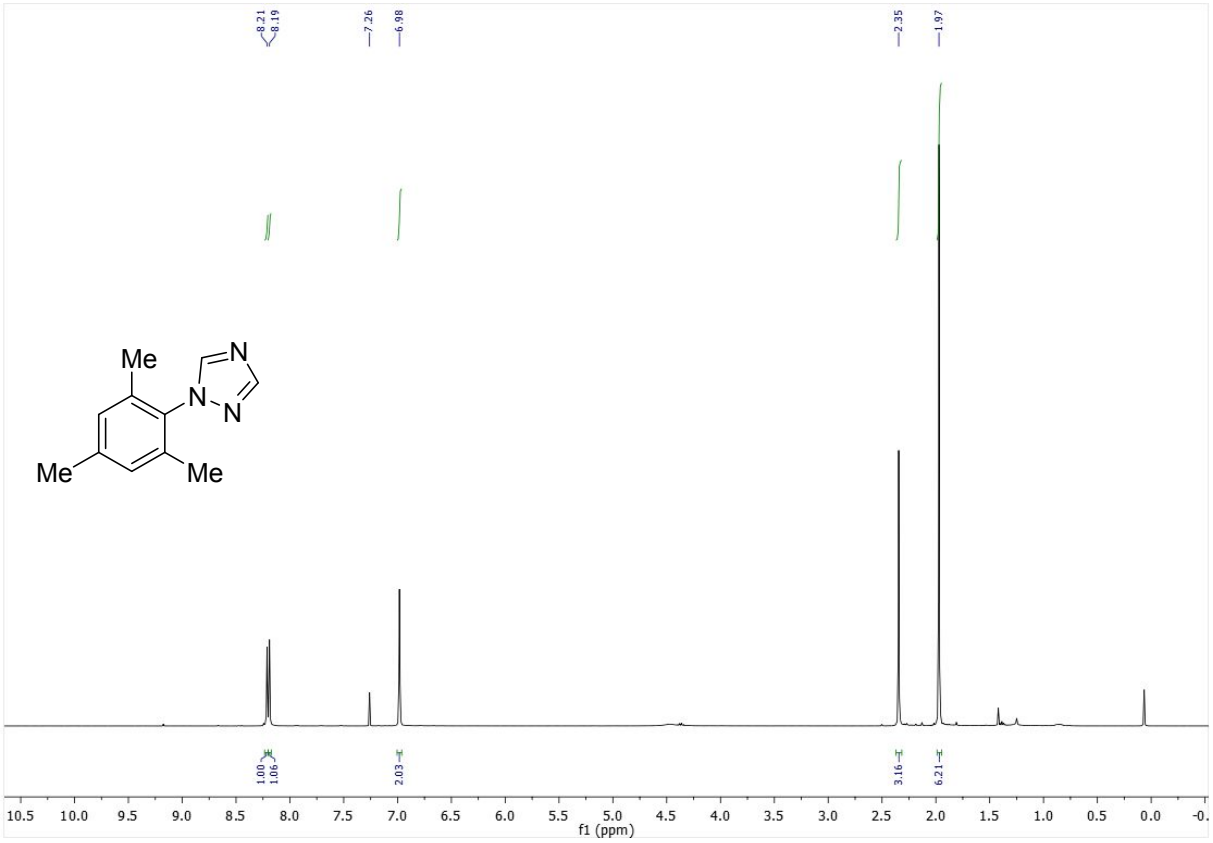

^{13}C{^{1}H} NMR (101 MHz, $CDCl_3$) (18)

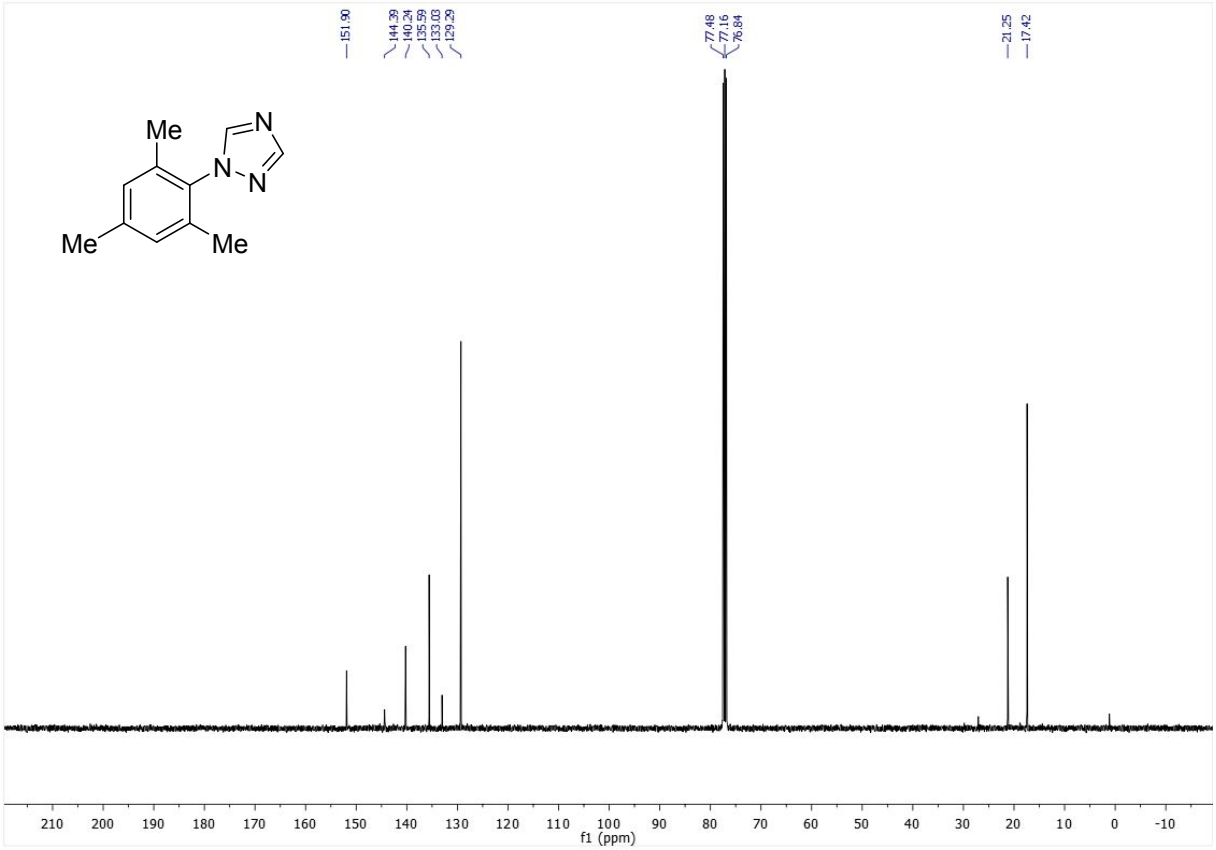

1-mesityl-1*H*-1,2,3-triazole (19) ^{1}H NMR (400 MHz, $CDCl_3$)

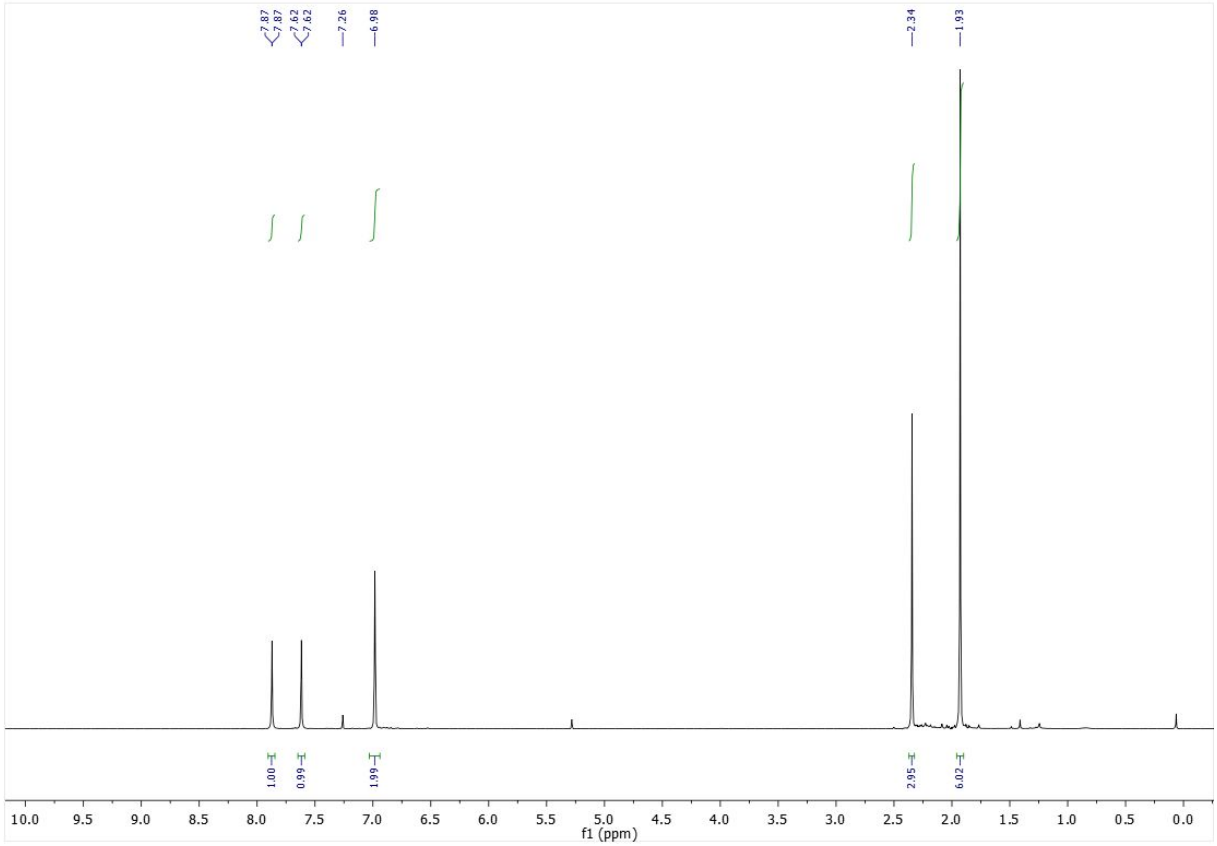

^{13}C{^{1}H} NMR (101 MHz, $CDCl_3$) (19)

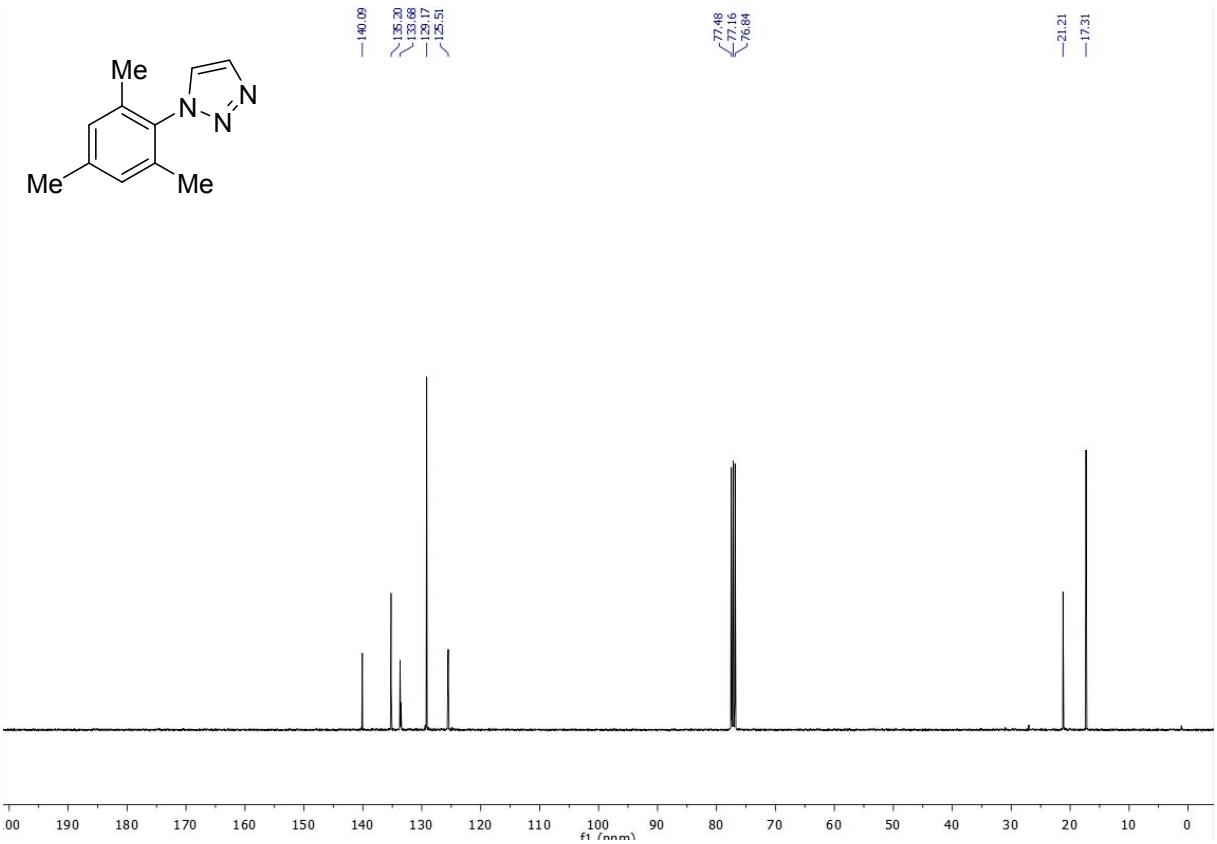

1-mesityl-1*H*-benzo[*d*]imidazole (20) ^{1}H NMR (400 MHz, $CDCl_3$)

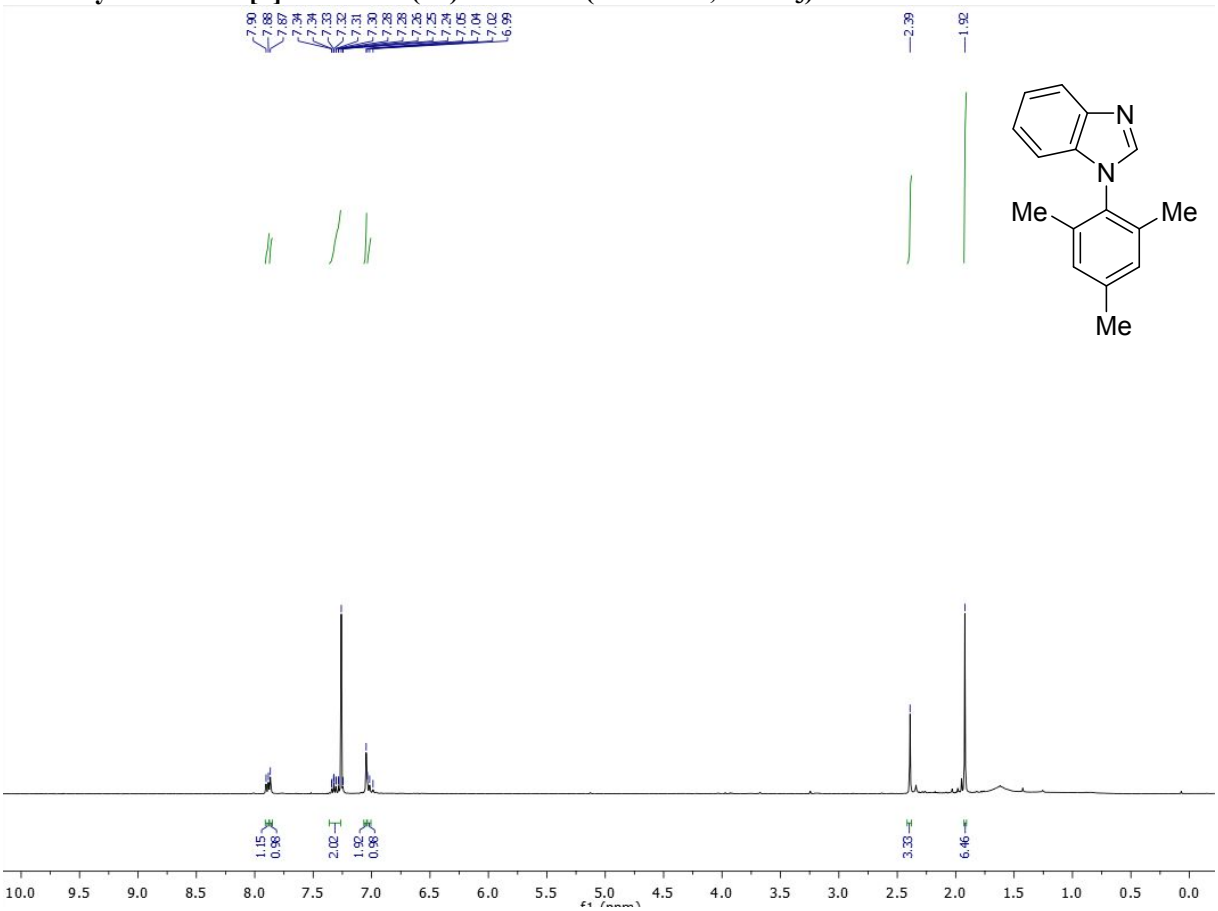

^{13}C{^{1}H} NMR (101 MHz, $CDCl_3$) (20)

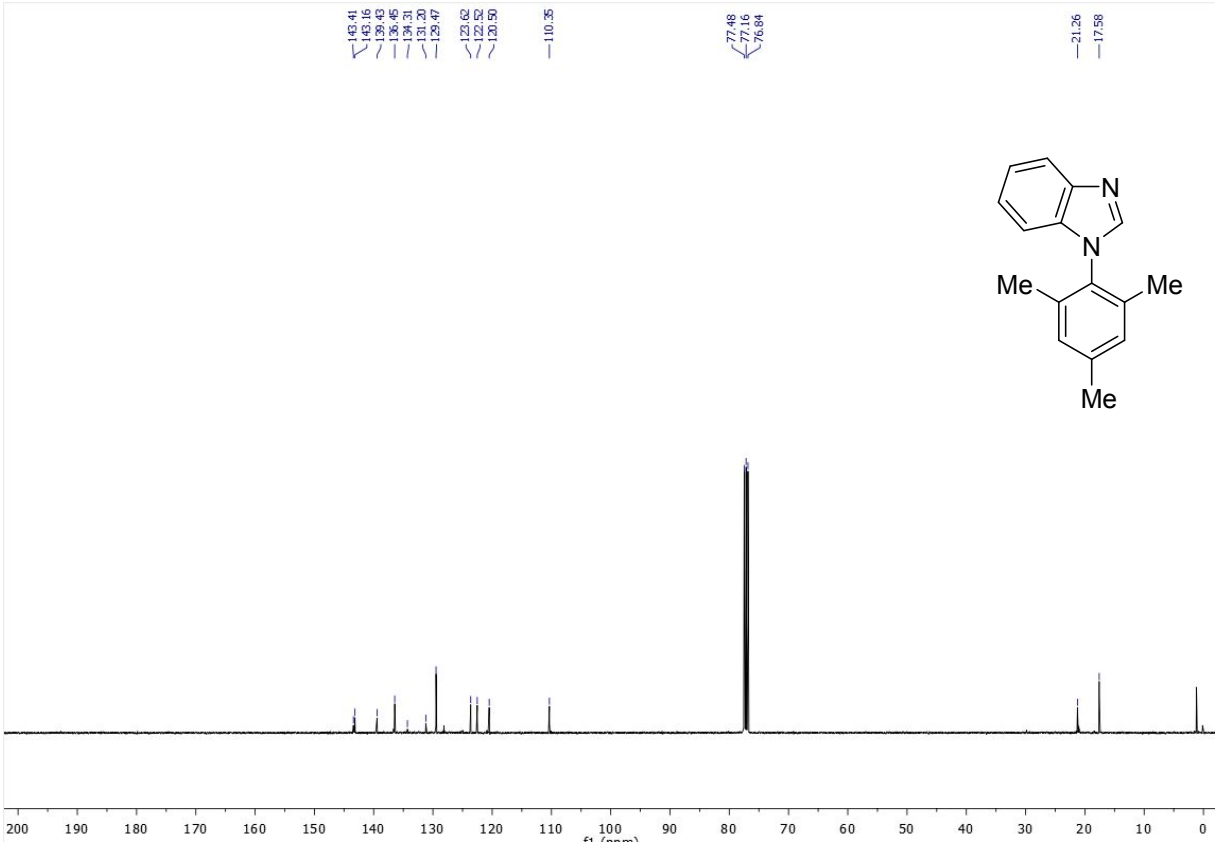

1-mesityl-1*H*-benzo[*d*][1,2,3]triazole (21) ^{1}H NMR (400 MHz, $CDCl_3$)

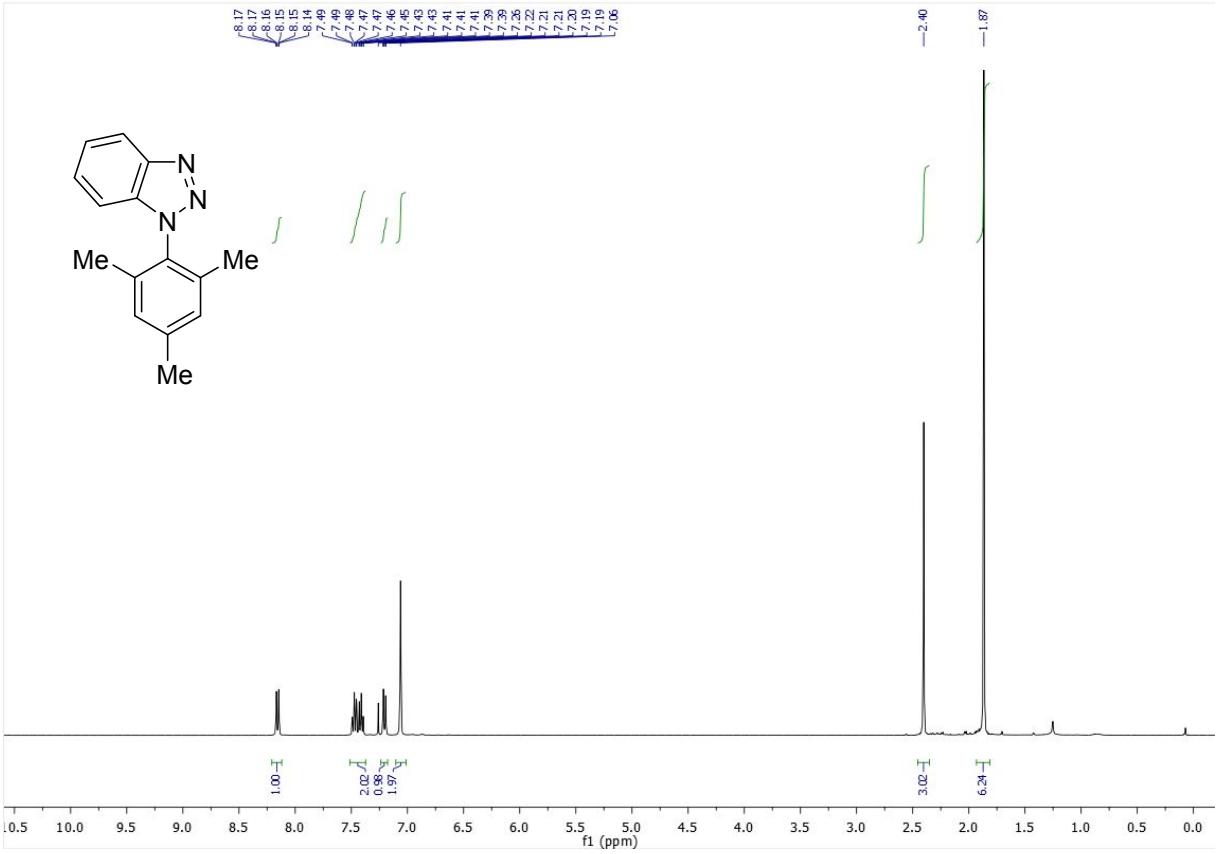

^{13}C{^{1}H} NMR (101 MHz, $CDCl_3$) (21)

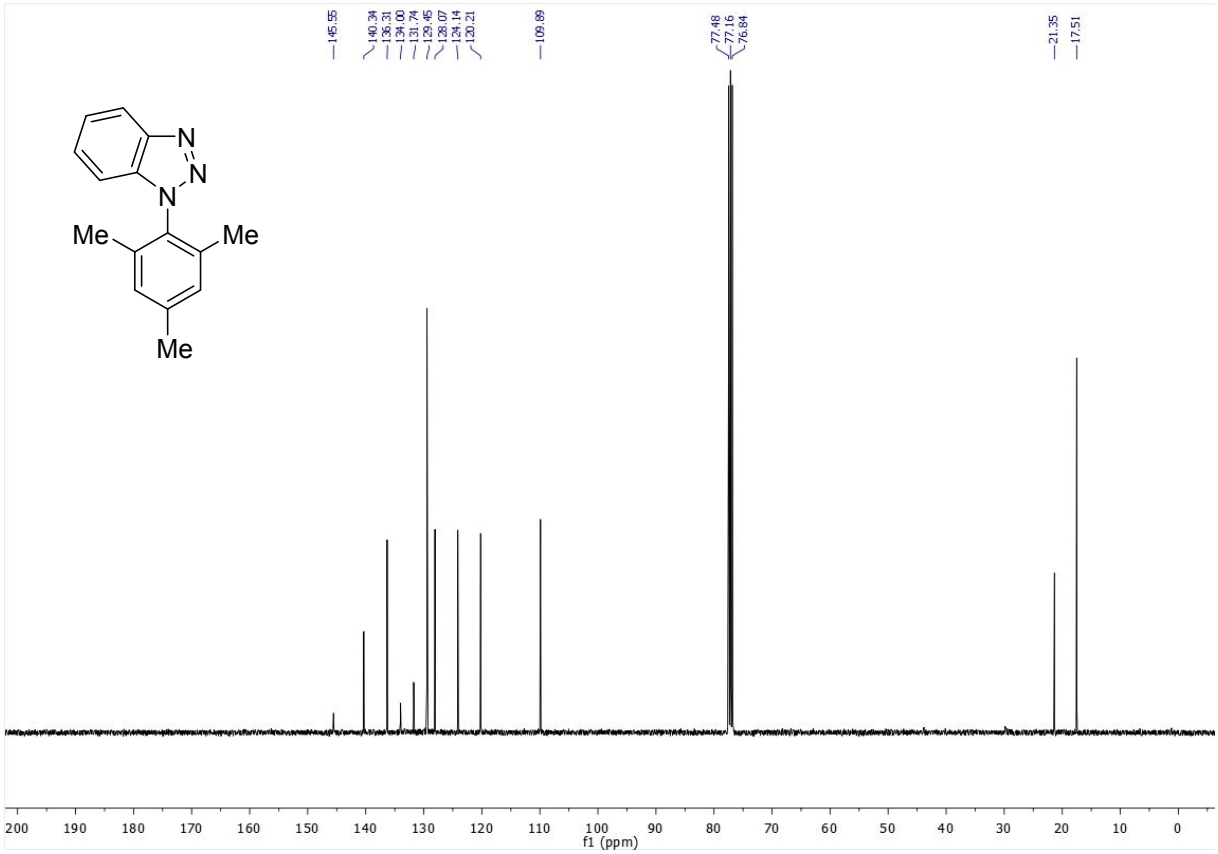

1-(2,5-di-*tert*-butylphenyl)-4-methyl-1*H*-pyrazole (22) ^{1}H NMR (400 MHz, $CDCl_3$)

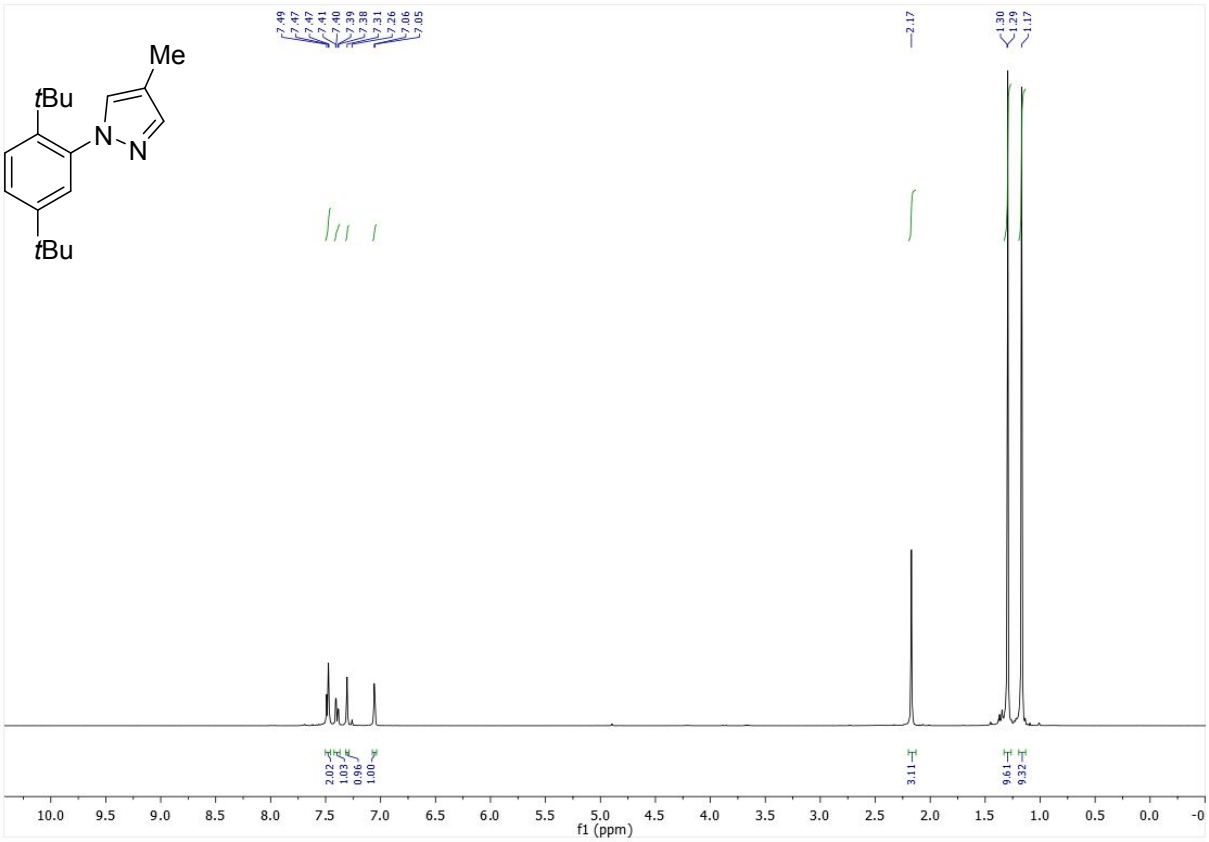

^{13}C{^{1}H} NMR (101 MHz, $CDCl_3$) (22)

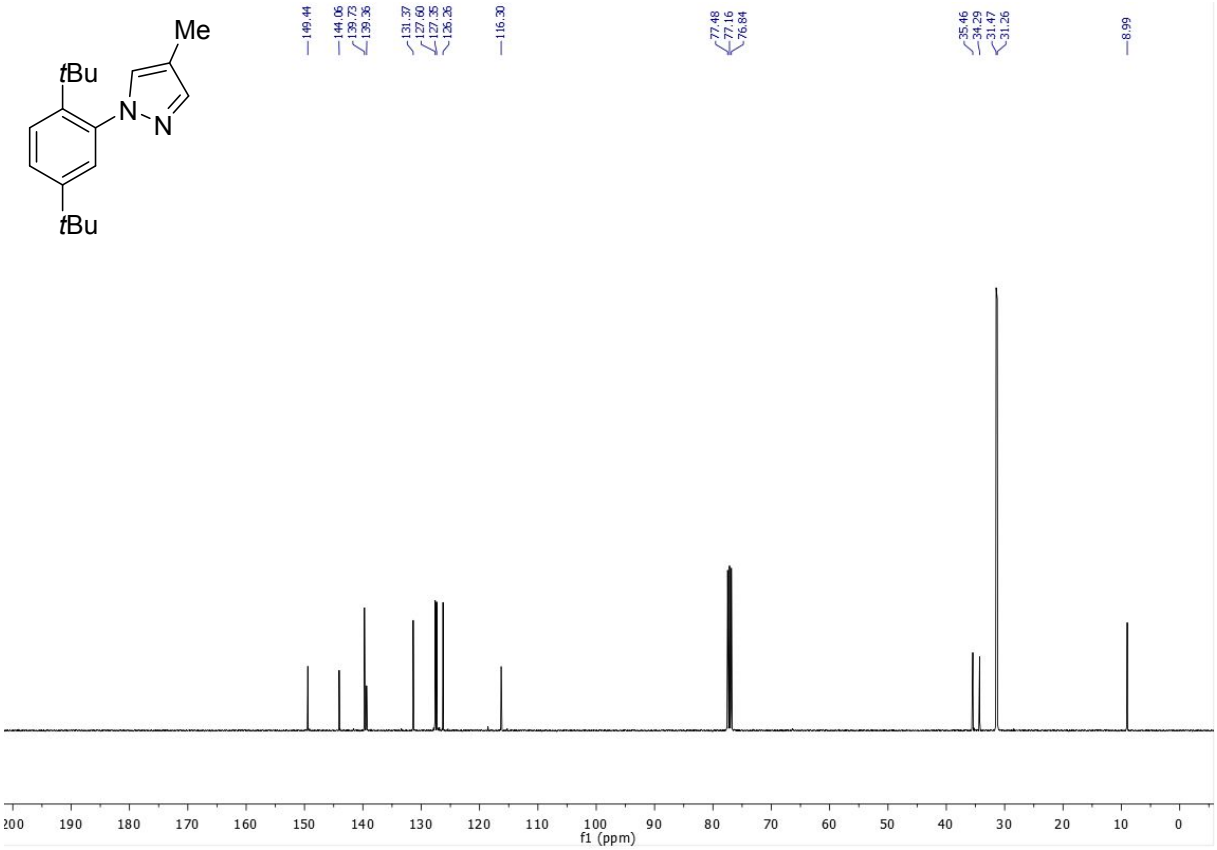

1-(2,5-di-*tert*-butylphenyl)-1*H*-1,2,3-triazole (23) ^{1}H NMR (400 MHz, $CDCl_3$)

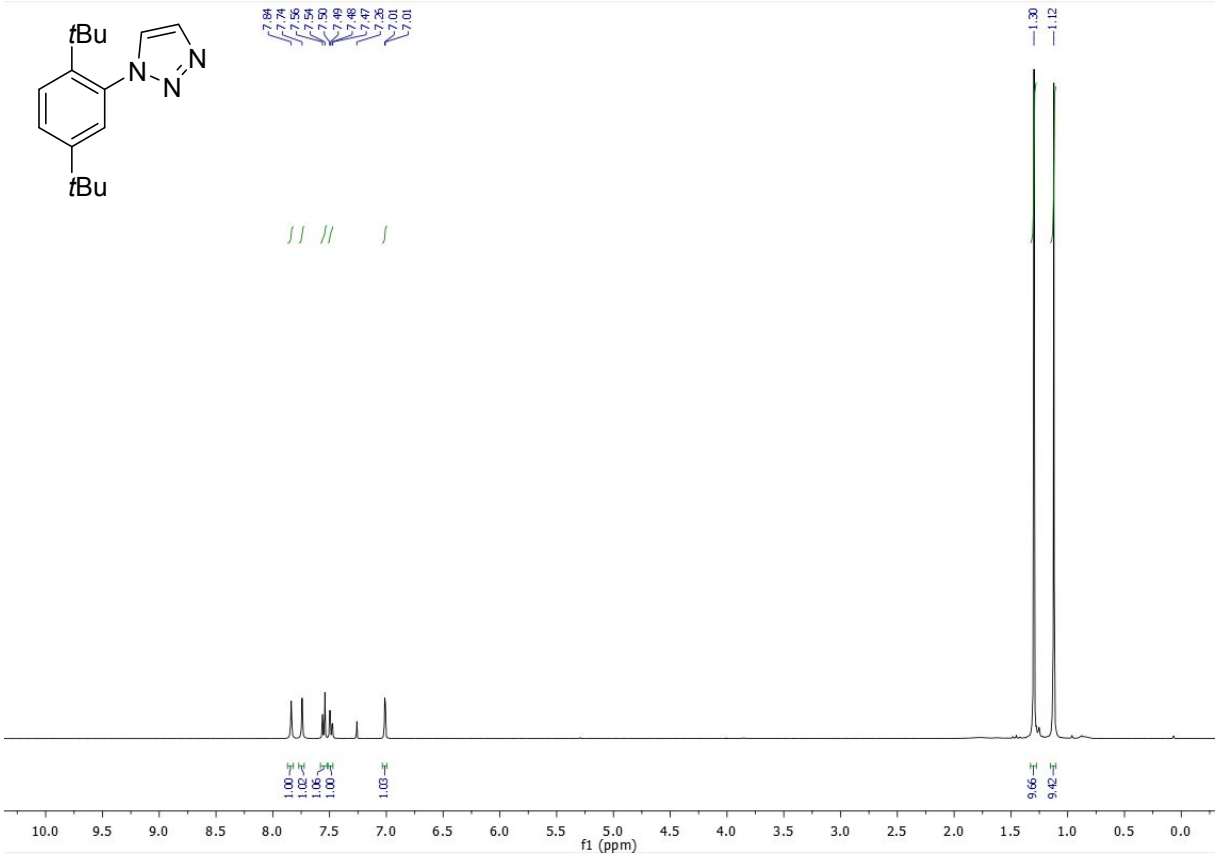

^{13}C{^{1}H} NMR (101 MHz, $CDCl_3$) (23)

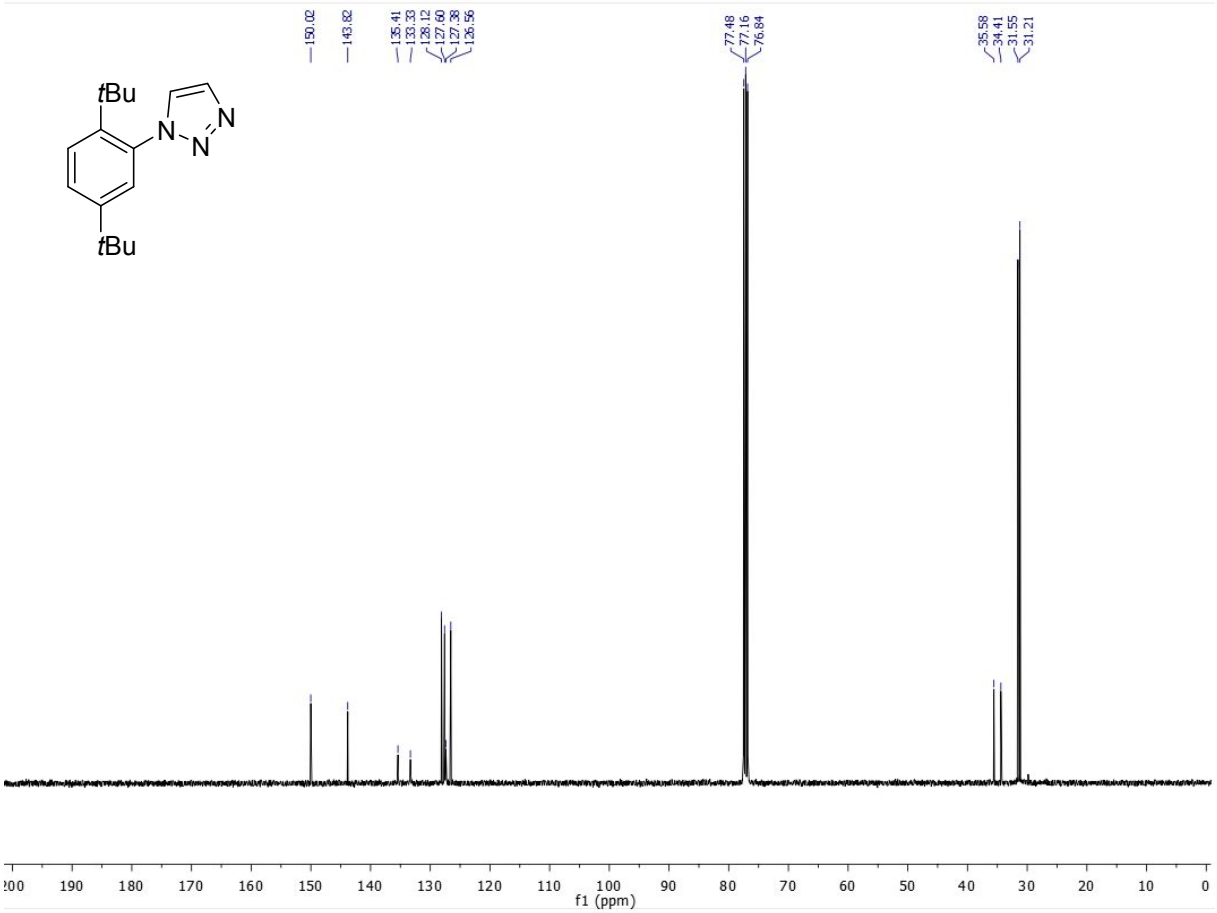

1-(2,5-di-*tert*-butylphenyl)-1*H*-benzo[d][1,2,3]triazole (24) ^{1}H NMR (400 MHz, $CDCl_3$)

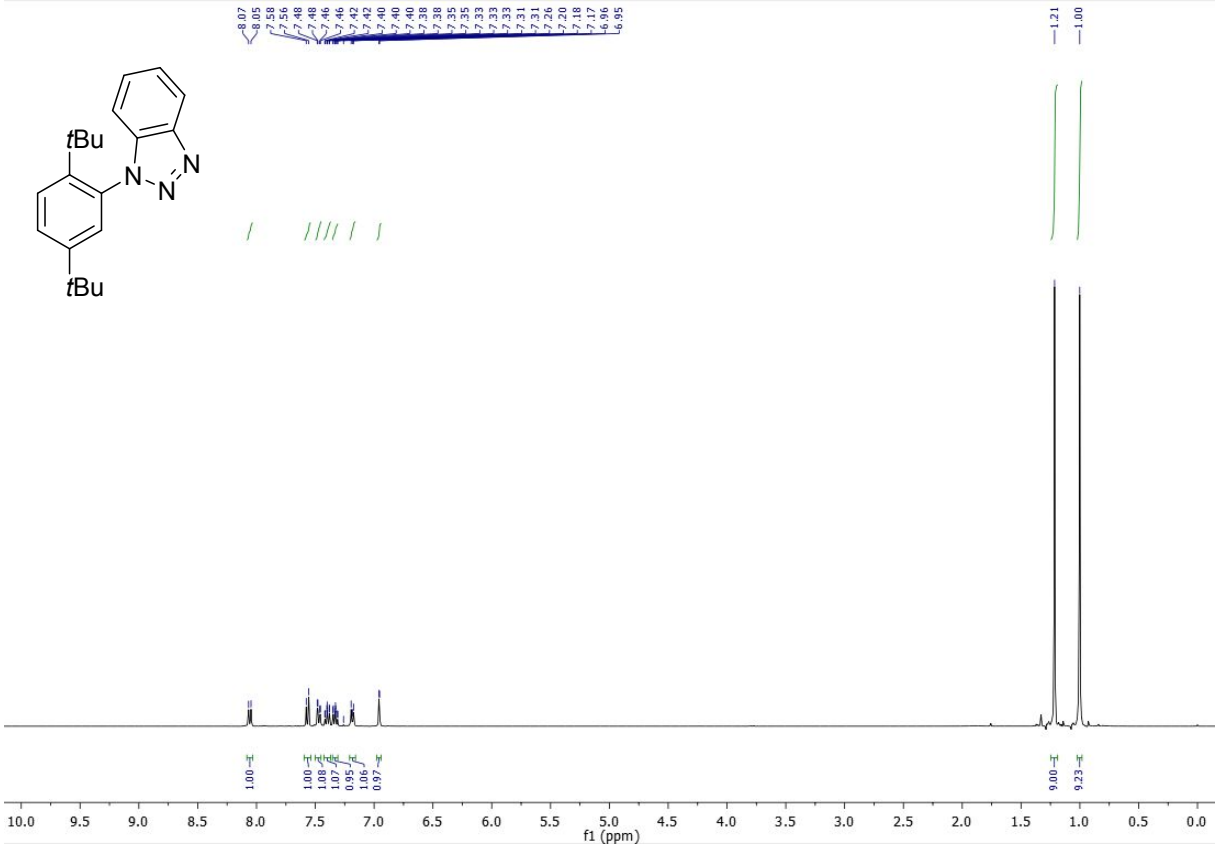

^{13}C{^{1}H} NMR (101 MHz, $CDCl_3$) (24)

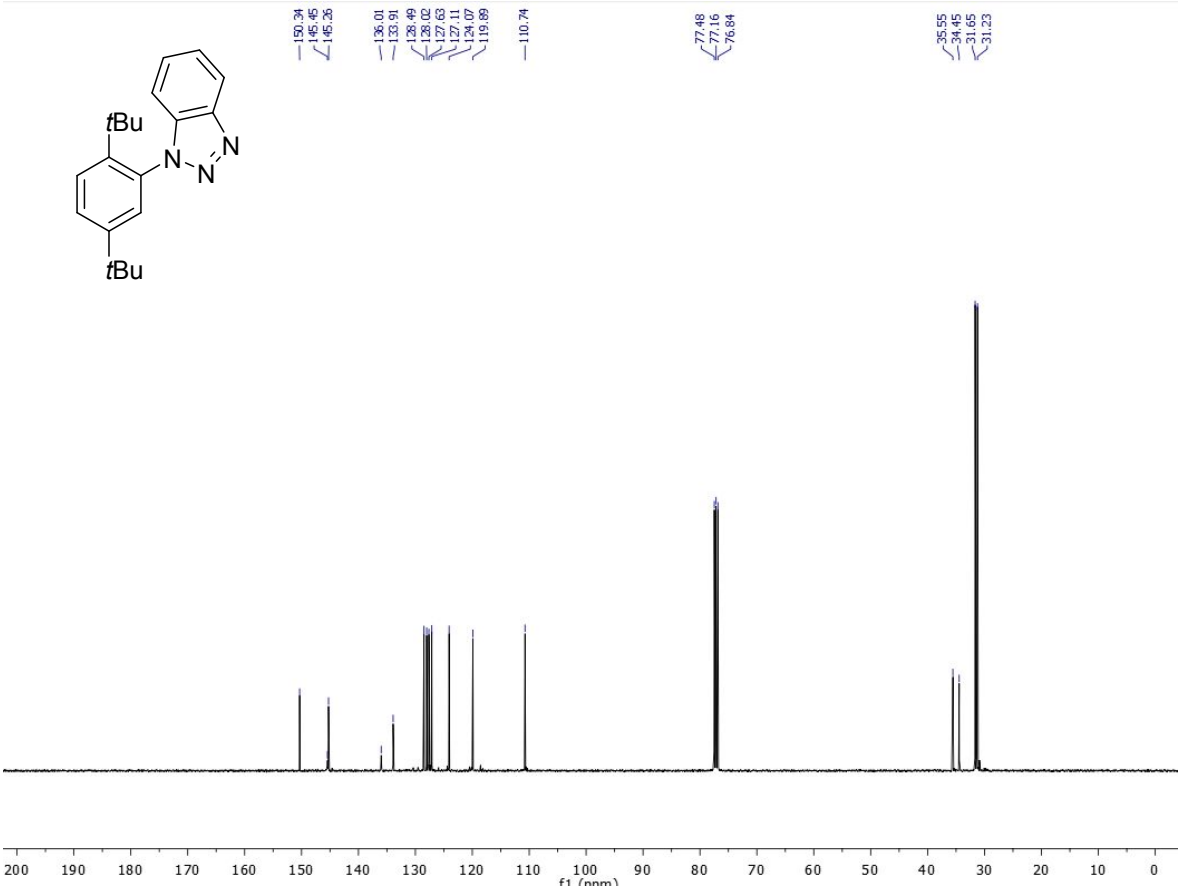

8. References

(1) Laudadio, G.; de Smet, W.; Struik, L.; Cao, Y.; Noël, T. Design and Application of a Modular and Scalable Electrochemical Flow Microreactor. *J. Flow Chem.* **2018**, *8* (3–4), 157–165. https://doi.org/10.1007/s41981-018-0024-3.

(2) Röckl, J. L.; Dörr, M.; Waldvogel, S. R. Electrosynthesis 2.0 in 1,1,1,3,3,3-Hexafluoroisopropanol/Amine Mixtures. *ChemElectroChem* **2020**, *7* (18), 3686–3694. https://doi.org/10.1002/celc.202000761.